universität wien

# MASTERARBEIT | MASTER'S THESIS

Titel | Title

Fundamental and Dominant Frequency in Bird Vocalizations: A Comparative Analysis

verfasst von | submitted by

Saskia Hagemann

angestrebter akademischer Grad | in partial fulfilment of the requirements for the degree of

Master of Science (MSc)

Wien | Vienna, 2025

| | |
|---|---|
| Studienkennzahl lt. Studienblatt \| Degree programme code as it appears on the student record sheet: | UA 066 878 |
| Studienrichtung lt. Studienblatt \| Degree programme as it appears on the student record sheet: | Masterstudium Verhaltens-, Neuro- und Kognitionsbiologie |
| Betreut von \| Supervisor: | Univ.-Prof. William Tecumseh Sherman Fitch PhD |

# Table of Contents

## Acknowledgments

I want to thank Professor W. Tecumseh Fitch for the opportunity to work on this project and thereby deepen my understanding of the methodological framework of bioacoustics research. I am very grateful for all the input and insights I received while being part of his research group, as well as for all the opportunities he provided to expand my knowledge and build connections in this field.

I am also deeply thankful to Christian Herbst for his advice and conceptual support throughout the project. His strong interest in my topic gave me confidence and provided a great motivational boost. I also thank to Jozsef Arato for providing code that was essential in building the analytical framework.

I would further like to thank all members of the research group for the warm and welcoming atmosphere, the fruitful discussions, and the support during the project. It was a great experience to be part the team.

A very special thanks goes to Sebastian Hochwallner, who supported me in every possible way, kept my back clear when needed, and reminded me to recharge my batteries. Finally, I would like to thank my dad, my brother, and the rest of my family for believing in me and encouraging throughout this journey.

# Abstract

The production of vocal sound in birds is highly diverse and shaped by the morphological variability of the syrinx, their unique vocal organ, and the vocal tract. This study investigates the relationship between fundamental frequency ($f_0$) and dominant frequency (DF) in bird vocalizations, aiming to clarify the correspondence between these two key acoustic parameters. Although $f_0$ and DF often are the same, they differ in a significant number of species, indicating that they cannot be used interchangeably and should not be conflated. Two datasets were analysed: (1) vocalizations (songs and calls) from 100 Passerines species and (2) calls from 100 species spanning 20 avian families. Using Fourier-based and autocorrelation-based methods, both $f_0$ and DF were extracted and compared across species; in addition, vocalization types (songs vs. calls) were compared within Passerines.

In Passerines, songs and calls exhibited similar mean $f_0$ values, while DF differed significantly, confirming that $f_0$ and DF reflect distinct aspects of vocal production. In the broader avian dataset, DF was significantly higher than $f_0$ across most families, although overlap between the two measures varied by taxon. Morphological traits such as body mass and beak size were included to explore potential physical influences on frequency parameters. Additionally, the influence of phylogenetic relatedness on acoustic parameters was considered.

The findings highlight that DF and $f_0$, while often related, are not interchangeable measures. A clear distinction between these parameters is essential for accurately interpreting the acoustic signals of birds, particularly in studies linking vocal traits to biological or ecological functions.

# Zusammenfassung

Vögel produzieren eine große Bandbreite verschiedener Vokalisationen, welche durch die morphologische Vielfalt des Syrinx – dem für Vögel einzigartigen Vokalorgan – und dem Vokaltrakt geformt werden. Die vorliegende Arbeit untersucht die Beziehung zwischen der fundamentalen Frequenz ($f_0$) und der dominanten Frequenz (DF) in Vogelvokalisationen, mit dem Ziel, das Zusammenspiel dieser beiden akustischen Schlüsselparametern zu klären. Obwohl sich $f_0$ und DF oft entsprechen, gibt es in einer Vielzahl an Spezies einen signifikanten unterschied zwischen ihnen, weshalb eine klare Differenzierung von großer Bedeutung ist. Für diese Arbeit wurden zwei Datensätze analysiert: (1) Vokalisationen (Gesang und Rufe) von 100 Passerines Arten und (2) Rufe von 100 Arten, die 20 unterschiedliche Vogelfamilien umspannen. Basierend auf Fourier-Transformation und Autokorrelation wurden $f_0$ und DF extrahiert und über die verschiedenen Arten miteinander verglichen. Zusätzlich dazu wurden die Vokalisationstypen – Gesang und Rufe – innerhalb der Passerines verglichen.

Innerhalb der Passerines zeigten Gesang und Rufe ähnliche Werte für $f_0$, unterschieden sich aber signifikant zwischen den DF Werten, was bestätigt, dass $f_0$ und DF unterschiedliche Aspekte der Lauterzeugung reflektieren. Innerhalb des breiter angelegten Datensatzes, war DF bei den meisten Familien signifikant höher als $f_0$. Morphologische Merkmale, wie Körper- und Schnabelgröße wurden ebenfalls einbezogen, um den möglichen Einfluss physischer Komponenten auf die Frequenzparameter zu untersuchen. Darüber hinaus wurde die Auswirkung verwandtschaftlicher Nähe auf die Ausprägung von Unterschieden zwischen den Arten bezüglich der akustischen Parameter miteinbezogen.

Die Resultate betonen, dass DF und $f_0$, wenngleich in der Regel eng verknüpft, sie einander nicht entsprechen. Eine klare Unterscheidung dieser beiden Messgrößen ist essentiell für eine akkurate Interpretation akustischer Signale in Vögeln, vor allem in Studien, die vokale Merkmale mit biologischen oder ökologischen Bedingungen in Beziehung setzen wollen.

# 1. Introduction

The basic procedure of producing vocal sound starts with an airflow coming from the respiratory system, passing the vocal tissues, positioned at the larynx (e.g. mammals) or the syrinx (birds), which leads to an opening and closing period of those membranes in a quasiperiodic way. The rate at which the vocal tissues vibrate defines the fundamental frequency ($f_0$). The produced non-sinusoidal sound wave consists of a $f_0$ and its upper harmonics, which are integer multiples of $f_0$. In an unmodified system the $f_0$ has the highest amplitude among all frequencies, followed by a gradual decline of the energy in the upper harmonics. Changes in subglottal pressure or vocal fold membrane tension (controlled by muscles) modulate $f_0$. (e.g. Herbst et al., 2025; Hopp et al., 1998)

According to the source-filter theory, the sound wave produced at the source propagates through the vocal tract, where a filtering process can take place (Herbst et al., 2025). In a non-static system, the shape of the resonance cavities in the vocal tract can be altered and support different frequencies depending on the shape of the cavities. This can lead to a change in the energy distribution, changing the spectral amplitude contour and thus carrying additional information. The frequency with the highest amplitude in the spectrum of a produced vocal sound is defined here as the dominant frequency (DF). (e.g. Herbst et al., 2025; Hopp et al., 1998)

This concept has been extensively studied in humans to gain insight into the mechanisms underlying speech and language. Similarly, birdsong has fascinated scientists for decades as a model system for investigating the bases of vocal learning and production. Although many knowledge gaps have been closed, new questions continue to arise. This study aims to contribute to this growing knowledge about bird vocalization and vocal production.

An important methodological aspect in this context concerns how vocal frequency is measured. In many bioacoustics studies, DF is used as a proxy for $f_0$, primarily because DF can be extracted more easily and reliably. Gingras et al. (2013) demonstrated in anuran vocalizations that these two frequencies are not in all cases interchangeable, highlighting that DF does not necessarily coincide with $f_0$. Here, this distinction is analysed in the context of avian vocal diversity.

## 1.1 Bird vocalizations

Bird vocalizations display remarkable diversity (Elemans et al., 2003). They vary across orders and species in terms of bandwidth, frequency range, and vocal flexibility (e.g. Elemans et al., 2003). One important distinguishing feature is the vocalization type – call versus song. Calls are generally short and simple, often used in contexts such as alarm signalling or social contact (e.g., Catchpole, 2008; Marler, 2004). Songs, by contrast, tend to be tonal, long, and complex, and are commonly associated with territory defence and mate attraction (e.g., Catchpole, 2008; Suthers, 2004). However, a clear classification is not always possible. This distinction is particularly relevant in the order Passeriformes, where vocal learning plays a prominent role in many species particularly in song. (e.g., Catchpole, 2008; Marler, 2004; Suthers, 2004)

The source of sound production in birds is the syrinx. It sits at the bottom of the trachea and is connected to air sacs (King, 1989 as cited in Elemans et al., 2015). It is characterized by high morphological diversity in shape and structure over the avian kingdom, and therefore results in a wide variety of sounds birds are capable of producing (Elemans, 2014). Many bird species possess two sound sources in the syrinx, and some taxa (e.g. songbirds) show bilateral independence, allowing simultaneous or alternating use of both sides (Suthers, 1990).

The sound produced by the syrinx can be modified in the vocal tract, which was first proven by Nowicki (1987) in his Helium experiment. Since then, several mechanisms have been identified by which birds filter the produced frequencies, such as tracheal elongation (Fitch, 1999) , tongue movement (Patterson & Pepperberg, 1994), or the opening and closing of the beak (Hoese et al., 2000). Riede et al. (2006) further showed that songbirds actively tune the resonance of their oropharyngeal-esophageal cavity to match $f_0$ of the song, thereby amplifying $f_0$ and suppressing higher harmonics. This raises the question of how such modulation mechanisms influence key acoustic parameters such as $f_0$ and DF over the class of birds, and whether these frequencies consistently reflect the same aspects of sound production.

The goal of this study was to investigate the relationship of the $f_0$ and the DF in bird vocalizations. The study addressed two levels of comparison. First, I quantified differences between the vocalization types song and call. This was examined among 100

different Passeriformes species of the suborder Passerines. Second, intra- and interspecific variation were compared by using calls of 100 species out of 20 different avian families representing the broader phylogenetic diversity of birds. Morphological parameters such as body mass and beak size, which are known to affect sound production and resonance frequencies (e.g., Demery et al., 2021; Huber & Podos, 2006), were included as potential predictors of acoustic variation. Finally, phylogenetic relatedness was accounted for, because closely related species are not statistically independent (Felsenstein, 1985).

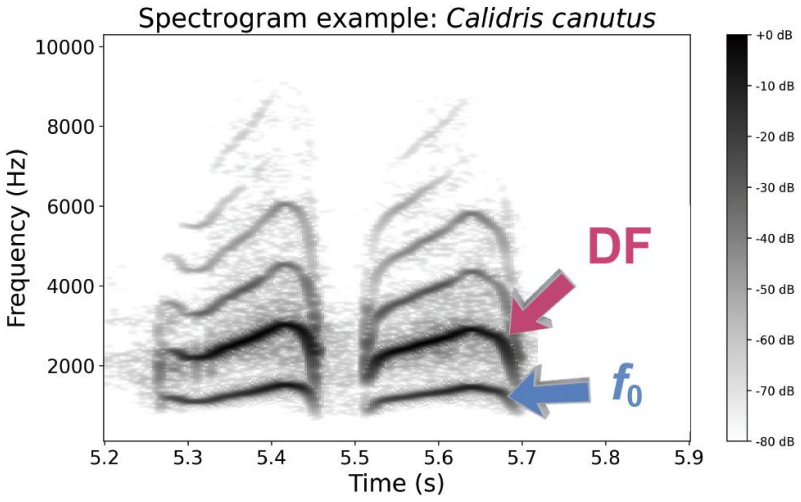


**Figure 1** Example spectrogram of a call of *Calidris canutus,* illustrating the fundamental frequency ($f_0$) and dominant frequency (DF). In this case, DF corresponds to an upper harmonic.

The study aimed to determine whether there are fundamental differences in the use or structure of $f_0$ and DF in Passerines compared to other avian orders and whether DF is a valid proxy for $f_0$ in the analysis of bird vocalizations, or whether these measures reflect distinct aspects of vocal production. Specifically, the study examines whether DF accurately represents $f_0$ across species and vocalization types, whether songs and calls differ in this relationship, and whether morphological traits or phylogenetic relatedness explain systematic variation between $f_0$ and DF.

It was expected to find cases where the DF is higher than $f_0$ and that this correspondence varies depending on vocalization type and morphological traits.

By combining acoustic measurements, morphological data, and phylogenetic analysis, this study aims to contribute to a more accurate and nuanced interpretation of vocal frequency parameters in birds and to clarify the methodological implications of using DF as a surrogate for $f_0$.

# 2. Material and Methods

## 2.1 Material

The analysis was based on audio recordings of bird vocalizations obtained from the 'Vogelstimmen' collection curated by A. Schulze (2003). This database contains high-quality WAV files of 819 different bird species from Europe, North Africa and Middle East.

For morphometric comparisons, values for body mass and beak dimensions were retrieved from the AVONET database (Tobias et al., 2022), which provides standardized morphological and ecological trait data for all bird species globally.

To account for phylogenetic non-independence between species, a dated phylogenetic tree was downloaded from birdtree.org (Jetz et al., 2012).

The processing and analyses of the data were performed using PRAAT (Version 5.3.61; Boersma & Weenink, 2013), Python (Version 3.11.4), and R (Version 4.2.1; R Core Team, 2022).

## 2.2 Data Preprocessing

All audio files were manually inspected and annotated using PRAAT. TextGrid annotation files were created, incorporating metadata provided by the 'Vogelstimmen' database (species name, vocalization type, life stages, sex if available) and a signal quality assessment for each of the individual recordings for any species. The annotation was conducted jointly by the author and a colleague.

Each file consisted either of a single recording or of multiple concatenated recordings. Each individual recording within a file was rated on a scale from 0 to 3, with 3 indicating the single recording with the highest signal quality in terms of signal-to-noise ratio and lack of background sounds. Exactly one quality-3 segment was present per file and was selected for further analysis. In cases where $f_0$ detection failed for the quality-3 segment – e.g., due to harsh on-tonal signal – a quality-2 segment from the same file was used as a fallback. Thus, a single vocalization exemplar was used for each species and / or vocalization type.

### 2.2.1 Filtering and Selection Criteria

Recordings of non-adult individuals, subspecies, and non-vocal sounds (e.g. bill clacks, wing flaps) were excluded from the database. Two datasets were created. A 'Passerines' dataset with 100 different passerine species, each represented by both a song and a call recording, and an 'All Birds' dataset, with calls of 100 different species spanning over 20 avian families, with five species per family.

Species were randomly selected using Python's 'random' package ('Passerines' n = 150, 'All Birds' Families with n > 6). Individual recordings were then manually reviewed and selected based on feasibility of $f_0$ detection , until a final set of 100 species was assembled for each dataset. Some files must have been affected by filtering during recording which affected in some cases the lowest detectable frequency (13 species in 'All Birds', 16 species in 'Passerines') – those had to be exchanged due to falsification of the measured amplitude.

**Table 1** Overview of the used datasets, including the species sample size (n) per dataset and the represented vocalization type.

| Dataset Overview | | |
|---|---|---|
| **Dataset** | **Subset** | **Vocalization type** |
| All Birds (n = 100) | | Calls |
| | Passerines (n = 40); (= "Pass") | Calls |
| | non-Passerines (n = 60); (= "noPass") | Calls |
| Passerines (n = 100) | | Calls and Songs |
| | Passerines Call (n = 100) | Calls |
| | Passerines Song (n = 100) | Songs |

## 2.3 Data Processing

### 2.3.1 Audio Preprocessing

All audio files were processed using Python. The annotations created in PRAAT were imported into Python using a custom script and transformed into a structured table ('pandas' (version 2.2.3; McKinney, 2010) DataFrame) containing start and end times, quality level, metadata, and filename. This table formed the basis for subsequent signal processing and analysis.

A custom Python script was developed to generate a spectrogram for each recording individually. For consistency, each file was resampled to a fixed sample rate of 44,100

Hz using ‘librosa’ (version 0.10.2; McFee et al., 2015)). A 4$^{th}$-order Butterworth bandpass filter (implemented with ‘scipy.signal’ from the ‘scipy’ package (version 1.15.3; Virtanen et al., 2020)) was applied to each recording. The cutoff frequencies were adjusted using pitch floor (fmin) and pitch ceiling (fmax) parameters, set via interactive sliders during spectrogram generation (see section 2.3.2). This ensured that the bandpass covered the expected vocal frequency range of each species while excluding low-frequency background noise and high-frequency artefacts. To further reduce background noise, the filtered signal was processed using the ‘noisereduce’ package (version 3.0.3; Sainburg, 2019/2025). This cleaned signal was then used for all subsequent analyses.

### 2.3.2 Spectrogram Generation

Spectrograms were computed using a Short-Time Fourier Transform (STFT) via ‘librosa’, with a window length of 2048 samples and a hop length of 512 samples. Amplitude values were converted to a decibel (dB) scale using ‘librosa.amplitude_to_db’, with the maximum amplitude as reference. Interactive sliders were implemented using ‘ipywidgets’ (version 8.0.4) graphical user interface (GUI) to adjust settings such as ‘start time’, ‘end time’, ‘time step’, ‘fmax’ (pitch ceiling), ‘fmin’ (pitch floor), ‘top_db’ (silence threshold = non-silent intervals), ‘voicing threshold’, and ‘octave cost’ for each sample (see Fig. 2 and table 2). The code for the spectrogram with implemented GUI sliders was based on a code kindly provided by Joszef Arato.

The ‘top_db’ slider defined the sections of the audio file that were recognized as actual sound based on decibel intensity, thereby segmenting the recording into distinct sound intervals (referred to as “individual segments” hereafter). In cases where recordings were particularly long, a representative section was manually selected. This section was chosen to best reflect the vocal characteristics of the species while also allowing reliable $f_0$ detection. The selection prioritized clear signal structure, minimal background noise, and segment quality. For each species a minimum of 2 individual segments was used.

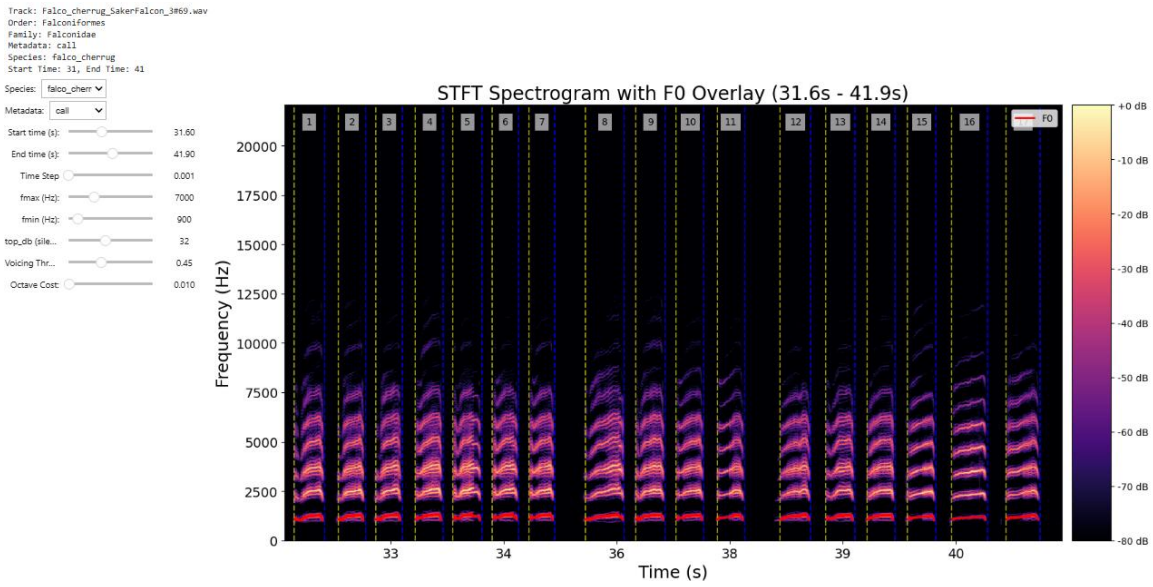


**Figure 2** Example spectrogram of a *Falco cherrug* call, generated using Python and illustrating the setup for the frequency extraction. The detected $f_0$ is shown as a red contour line. Brightness intensity reflects amplitude; thus the dominant frequency appears as the most prominent (brightest) horizontal band, in this case the first or second overtone of $f_0$. Visible on the left are the interactive sliders for individual adjustments of the settings for the current spectrogram.

**Table 2** GUI sliders used for adjustment of the displayed spectrogram and $f_0$ extraction.

| **Sliders** | **Definition** |
|---|---|
| Start time (s) | Start time of the manually selected signal section |
| End time (s) | End time of the manually selected signal section |
| Time step | Controls temporal resolution of $f_0$ tracking |
| fmax (Hz) | "pitch ceiling"; upper frequency boundaries for $f_0$ estimation; Default range: 400 – 22,050 Hz |
| fmin (Hz) | "pitch floor"; lower frequency boundaries for $f_0$ estimation; Default range: 10 – 8,000 Hz |
| top_db | Silence threshold (in dB) used to detect non-silent intervals |
| Voicing Threshold | Controls aperiodicity in the signal for a correct $f_0$ detection; basic setting: 0.45 |
| Octave Cost | Supports subharmonic suppression for correct $f_0$ detection; basic setting: 0.01 |

### 2.3.3 $f_0$ Detection

$f_0$ was detected using the autocorrelation algorithm of PRAAT. The 'voicing threshold' slider was used to control sensitivity to aperiodic sections in the signal. It was typically set to 0.45 (the default value in PRAAT), unless manual inspection showed detectable influence on a correct $f_0$ contour. The 'octave cost' slider helped suppress subharmonics

being spuriously detected as $f_0$. It was generally set to 0.01 unless higher values led to better results in ambiguous cases. (Boersma, 1996)

### 2.3.4 Frequency Extraction

Fundamental frequency ($f_0$) values ($f_0$-min , $f_0$-mean , $f_0$-max) were extracted using the autocorrelation method from the 'parselmouth' (version 0.4.4; Jadoul et al., 2018) package, which replicates the functionality of PRAAT. For each manually selected part of the signal, defined by start and end time and according to all adjusted sliders (fmin, fmax, time step, voicing threshold, octave cost) $f_0$ was extracted. The resulting $f_0$ contour was filtered in two steps: values below 90 Hz were excluded, as no species in the dataset produced $f_0$ in this range (lowest observed $f_0 \approx 250$ Hz). This threshold served to remove spurious pitch detections. Additionally, values with voicing strength below the defined threshold were discarded. Only time points located within the previously identified non-silent intervals were retained. This $f_0$ contour was visually checked to ensure it overlaid the $f_0$ in the spectrogram (see Fig. 2).

The dominant frequency (DF) was computed using a Fast Fourier Transform (FFT) implemented via the 'scipy.fft' module. For each individual segment one DF was computed.

For each species several individual segments were created by the 'tob_dB'-slider, for each individual segment acoustic parameters were extracted, including $f_0$-min , $f_0$-mean, $f_0$-max, and DF. To obtain comparable values, the segment-level measurements were aggregated: mean values of the $f_0$ and DF, as well as the absolute minimum and maximum values of $f_0$. These aggregated values served as the basis for the analyses in both datasets ("All Birds" and "Passerines").

### 2.3.5 Quality Control

Each spectrogram for every species sample was cross-checked visually in PRAAT using spectrograms and, for more complex cases, additional frequency spectra. As an additional validation step, a scatterplot was created in python to display the detected parameters ($f_0$-min , $f_0$-mean , $f_0$-max, DF) for each individual segment (see Fig. 3). This allowed assessment of whether $f_0$-mean and DF lay within the expected frequency range. In addition to visual inspection, all audio samples were listened to during manual quality control.

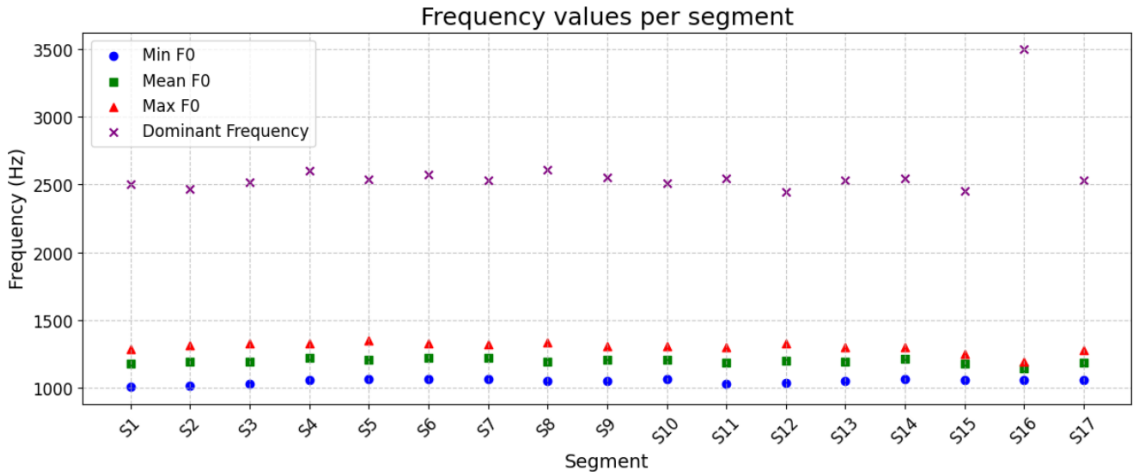


**Figure 3** Example scatterplot of the extracted frequency values ($f_0$-min , $f_0$-mean , $f_0$-max, DF) of *Falco cherrug*, used as additional control for the frequency extraction. The individual segments set by the top_dB slider are on the x-axis, the frequencies on the y-axis.

### 2.3.6 Phylogenetic Data Preparation

Phylogenetic analyses were conducted on the 'All Birds' (n = 100) dataset. For this purpose a consensus tree was generated based on a set of posterior trees from birdtree.org (Jetz et al., 2012), using the Hackett (Hackett et al., 2008) backbone and the sequenced species subset. This backbone was selected because it resulted in fewer polytomies in the consensus tree compared to alternative sets.

A set of 1,000 posterior trees was downloaded and processed in R using the 'phytools' (version 2.3.0; Revell, 2024) package. From these, a 50% majority-rule consensus tree was generated via the 'consensus.edge()' function.

The initial consensus tree contained 89 of the 100 species included in the original 'All Birds' dataset. The remaining 11 species were not represented in the Hackett sequenced species set and were therefore excluded from the phylogenetic analyses.

To ensure that the tree was fully bifurcating and suitable for analyses such as Phylogenetic Generalized Least Squares (PGLS), families with unresolved polytomies were removed. These included the families *Muscicapidae* and *Ardeidae*. The resulting pruned tree included 80 species.

To maintain balance in species representation across families, two additional families – *Charadriidae* (1 species) and *Rallidae* (2 species) – were excluded. The resulting tree included 77 species from 16 families, with each family represented by 4 or 5 species, ensuring consistency for comparative analyses.

The corresponding trait dataset was filtered accordingly to match the tree tips. The final tree was then validated using the 'phytools' and 'ape' (version 5.8; Paradis & Schliep, 2019) R packages. It was confirmed to be fully bifurcating, with no remaining polytomies (sum(polytomies) = 0), and not ultrametric, as minor differences in branch lengths were retained to reflect relative divergence among species. Given that PGLS under a Brownian motion model does not require an ultrametric tree, this was considered appropriate for the analyses. This finalized tree (see Appendix), together with the matched trait dataset, was subsequently used for the analysis of phylogenetic signal and in the PGLS models

## 2.4 Statistical Analyses

Statistical analyses included within-species comparison, as well as between-species correlation and regression models. The analyses focused on two main areas of interest: (1) the relationship between $f_0$ and DF across species and different vocalization types (calls and songs), and (2) the influence of morphological and phylogenetic factors on acoustic parameters.

Acoustic parameters included $f_0$-min , $f_0$-mean , $f_0$-max, DF (see table 3), while morphological parameters (sourced from the AVONET database) included body mass (in grams), beak length (culmen), beak width, and beak depth (see Figure 4).

**Table 3** Overview of acoustic parameters used in this study.

| **Acoustic Parameters** | |
|---|---|
| $f_0$ | Fundamental frequency (= vocal fold vibration rate) |
| $f_0$-min | Minimum $f_0$ within an individual or summary segment. |
| $f_0$-max | Maximum $f_0$ within an individual or summary segment. |
| $f_0$-mean | Mean $f_0$ within an individual or summary segment. |
| DF | Dominant frequency (= frequency with highest amplitude); extracted as the absolute value per individual segment |
| DF-mean | Mean of DF values across all individual segments of a species and vocalization type |

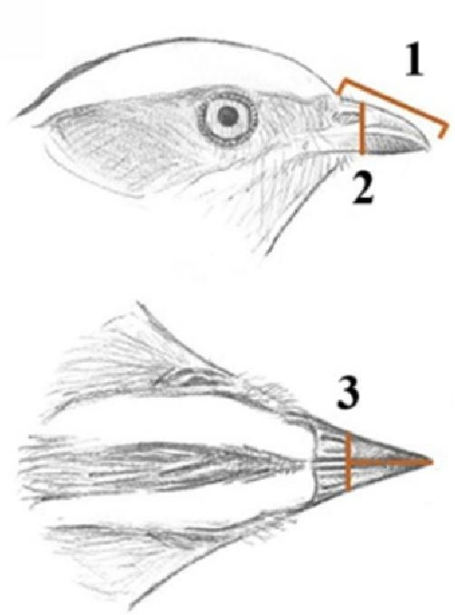


**Figure 4** Morphological parameters sourced from the AVONET database (Tobias et al., 2022): used Beak parameters: (1) beak length culmen, (2) beak depth, (3) beak width; *Picture adapted from Tobias et al. (2022)*

### 2.4.1 Classical Statistical Analyses

All the 'classical' statistical analyses were performed in Phython using the packages 'pandas' (version 2.2.3; McKinney, 2010), 'scipy' (version 1.15.3; Virtanen et al., 2020), 'statsmodels' (version 0.14.2; Seabold & Perktold, 2010), 'pingouin' (version 0.5.4; Vallat, 2018), and using 'matplotlib' (version 3.10.3; Hunter, 2007) / 'seaborn' (version 0.13.2; Waskom et al., 2023) for visualization. Before applying statistical tests, all variables were tested for normality using the Shapiro-Wilk test. If required, variables were transformed to meet test assumptions, with logarithmic ($\log_{10}$), square-root (sqrt), or no transformation (none) applied as appropriate.

To descriptively explore the frequency alignment between $f_0$ and DF within individual segments, the proportion of segments in which DF fell within the detected $f_0$-range (i.e., between $f_0$-min and $f_0$-max) was calculated. This analysis was performed for the 'All Birds' dataset and for the Passerines subsets calls and songs.

In a complementary approach, a ratio of DF to $f_0$-mean was calculated for every segment of each species. These ratios were used to examine whether DF corresponded to the $f_0$ itself (ratio ≈ 1), or to higher harmonics (e.g., 2 $f_0$, 3 $f_0$, etc.). The resulting values were

visualized as histograms for each dataset, allowing for a descriptive overview of harmonic patterns across species and vocalization types.

**Within-species analyses** were based on species-wise summary segments. To evaluate the relationship between $f_0$ and DF within the 'All Birds' dataset, its subsets 'Pass' and 'noPass' and for each vocalization type in the 'Passerines' dataset, paired t-tests were executed separately for calls ('All Birds' and 'Passerines Call') and songs ('Passerines Song'), comparing $f_0$-mean and DF-mean. Additionally, to compare acoustic differences between call and song within the same species of the 'Passerines' dataset, paired t-tests were performed on $f_0$-mean and DF-mean.

**Between-species analyses** focused on cross-species relationships between $f_0$ and DF, as well as on body mass vs $f_0$. Linear regressions were performed using species-wise summary values to test those relationships. These models were applied to the full 'All Birds' dataset (n = 100), as well as to its subsets comprising Passerines ('Pass'; n = 40) and non-Passerines ('noPass'; n = 60). In addition, within the 'Passerines' dataset separate regressions were run for calls and songs (each n = 100), comparing $f_0$-mean and DF-mean for each vocalization type. Model assumptions were assessed using Shapiro-Wilk tests and diagnostic plots (residuals, Q-Q plots). Minor deviations from normality were accepted when visual inspection indicated an otherwise robust model fit.

To explore associations between acoustic and morphological variables, correlation matrices were computed on summary segments for all frequency (min, mean, max values for $f_0$ and DF) and morphological parameters (body mass, beak length, width, and depth). To keep the analysis consistent and comparable the non-parametric Spearman rank method was applied across variables for all correlation matrices, as several morphological variables did not meet the assumptions of normality, even after $\log_{10}$ or square root transformation. For the beak parameters (length, width, depth) partial correlations with DF were performed to control for body mass.

### 2.4.2 Phylogenetic Analyses

To account for the shared evolutionary history of species, phylogenetic analyses were conducted on the filtered 'All Birds' dataset (n = 77 species) using a pruned consensus tree based on the Hackett backbone (see section 2.3.7). All analyses were performed in R, primarily using the packages 'nlme' (version 3.1.163; Pinheiro, 2011), 'phytools', and

‘geiger’ (2.0.11; Pennell et al., 2014). The code was based on code provided in the book ‘Phylogenetic Comparative Methods in R’ (Revell & Harmon, 2022; p. 61-70 and p. 84-98).

Phylogenetic signal was estimated for each acoustic and morphological trait using Blomberg’s K (Blomberg et al., 2003) and Pagel’s λ (Pagel, 1999). Blomberg’s K values were calculated using the phylosig() function from the ‘phytools’ package. Under a Brownian motion model (evolutionary “random walk” development (Revell & Harmon, 2022)), K = 1 is expected. Values < 1 indicate a weaker phylogenetic signal than expected, whereas values > 1 indicate a stronger signal than expected (Blomberg et al., 2003). Pagel’s λ was estimated by fitContinuous() from the ‘geiger’ package. Pagel’s λ measures how strongly the distribution of trait values follows the phylogenetic tree, with $\lambda = 0$ indicating no phylogenetic dependence and $\lambda = 1$ indicating the pattern under a Brownian motion (Pearse et al., 2025).

Phylogenetic Generalized Least Squares (PGLS) models were used to test the relationship between acoustic and morphological traits while accounting for the phylogenetic relatedness between species. For this, a Brownian motion model was applied (‘corBrownian’) based on the pruned species tree, and models were fitted using the ‘gls()’ function, from the ‘nlme’ package. To minimize multicollinearity among predictors, variance inflation factors (VIFs) were calculated from linear models, and predictors with high collinearity were excluded where necessary. Additionally, relative importance metrics were computed using the ‘relaimpo’ package (version 2.2.7; Grömping, 2006) to evaluate the proportion of variance explained by each predictor and to guide model selection for the PGLS analyses. Model residuals were assessed for normality using the Shapiro-Wilk test.

# 3. Results

## 3.1 Descriptive Analyses

The percentage of the individual segments in which DF was equal to $f_0$ was calculated for the 'All Birds' dataset, its subsets 'Pass' and 'noPass', and the two Passerines subsets (call and song).

DF corresponds to $f_0$ in 50.10% of all individual segments out of the 'All Birds' dataset, 38.81% in the 'All Birds – noPass' subset and 72.89% in the 'All Birds – Pass' subset. In the 'Passerines call' subset DF corresponds to $f_0$ in 85.47% of all individual segments and 95.31% in the 'Passerines song' subset. As a complementary approach, the distribution of DF values relative to $f_0$ and the upper harmonics was visualized by calculating the ratio DF / $f_0$ and plotting the resulting distribution as histograms (see Fig. 5).

The histograms reveal that DF most frequently corresponds to $f_0$. In the 'All Birds' dataset (Fig. 5A), a considerable proportion of DF values correspond to $2f_0$, and a few even align with higher harmonics. The two 'All Birds' subsets demonstrate that the highest proportion of DF corresponding to an upper harmonic fell into the non-Passerines subset (Fig. 5B). In contrast, the 'Passerines call' subset (Fig. 5D) shows far fewer cases of DF = $2f_0$ and only very few instances at $3f_0$. For songs (Fig. 5E), this pattern is most pronounced, with DF almost exclusively corresponding to $f_0$, and only a small fraction aligning with $2f_0$.

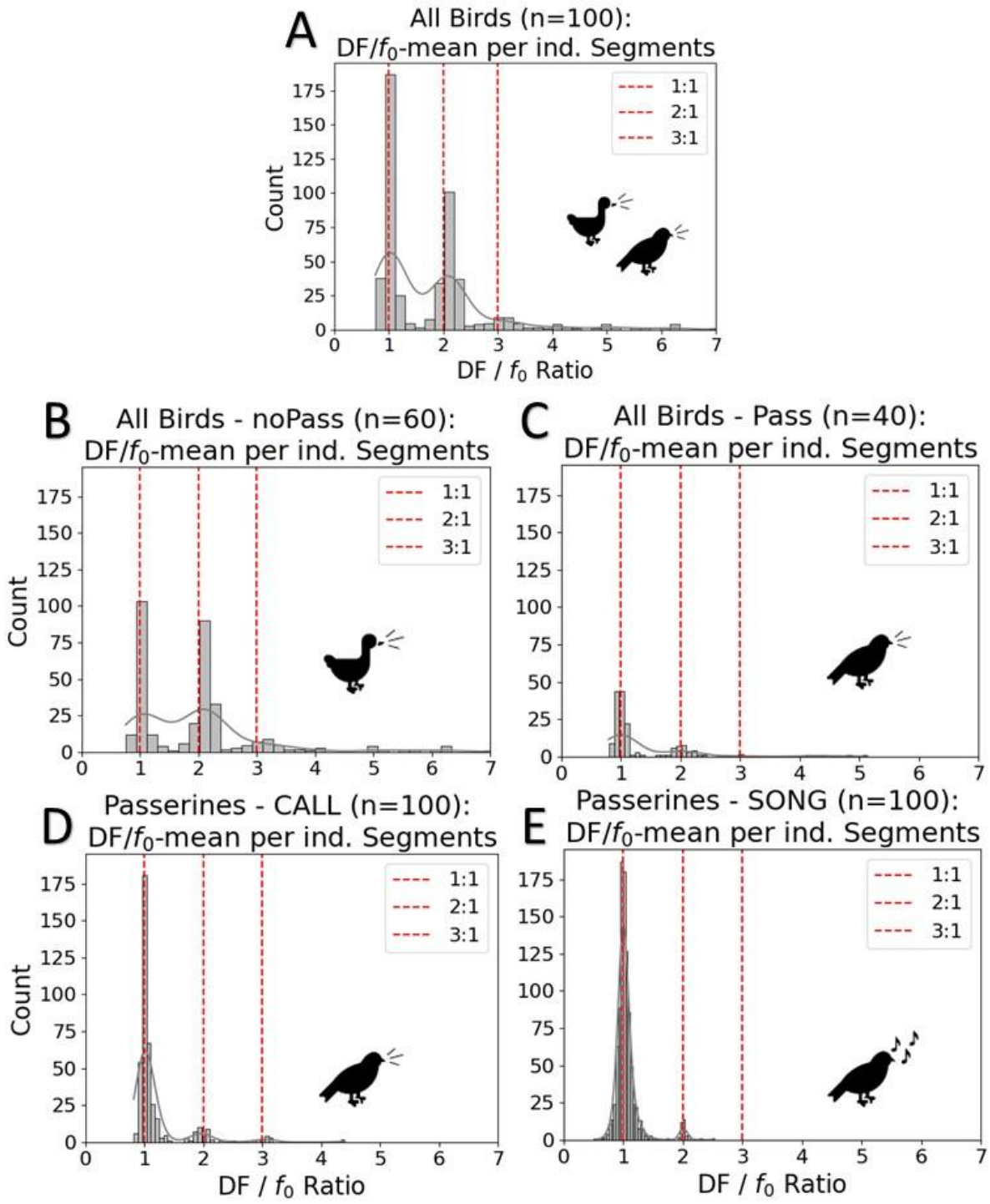


**Figure 5** Distribution of DF divided by $f_0$-mean values per individual segment for all datasets (A-E), representing the amount of cases when DF corresponds to either $f_0$ or an upper harmonic (2 $f_0$, 3 $f_0$, *et cetera*).

## 3.2 Paired comparisons

DF and $f_0$ extracted from the species-wise summary segments of each dataset were used for the t-tests. The frequency variables used in the t-tests met the assumption of normality after appropriate transformation (log, square root, or none, see table 4), as determined via Shapiro-Wilk test.

In the 'All Birds' dataset (n = 100), paired t-tests showed that DF was significantly higher than $f_0$ in calls (t = -9.09, p < 0.001, d = -0.91). This pattern held in both the non-Passerines subset 'noPass' (n = 60; t = -7.91, p < 0.001, d = -1.02) and the Passerines subset 'Pass' (n = 40; t = -3.77, p < 0.001, d = -0.60). The results of the $f_0$ and DF comparison of the 'Passerines call' dataset (n = 100; t = -5.17, p < 0.001), showed similar results to the 'Pass' subset. In contrast, song vocalizations showed a weaker difference between $f_0$ and DF (n = 100; t = -2.61, p = 0.01, d = -0.26).

A direct comparison between $f_0$ in calls and songs of Passerines showed no significant difference (t = -0.26, p = 0.798), while DF was significantly higher in calls compared to songs (t = 3.084, p = 0.003, d = 0.308). (see table 4 and Figure 6)

**Table 4** T-test results of all datasets.

| Dataset | Tranf. | Test | t-value | p-value | Cohen's d |
|---|---|---|---|---|---|
| All Birds | $\log_{10}$ | $f_0$ vs DF | -9.089 | <0.001 *** | -0.909 |
| All Birds - noPass | none | $f_0$ vs DF | -7.912 | <0.001 *** | -1.021 |
| All Birds - Pass | sqrt | $f_0$ vs DF | -3.768 | <0.001 *** | -0.596 |
| Passerines Call | sqrt | $f_0$ vs DF – Call | -5.170 | <0.001 *** | -0.517 |
| Passerines Song | $\log_{10}$ | $f_0$ vs DF – Song | -2.611 | 0.010 * | -0.261 |
| Passerines | sqrt | Call vs Song – $f_0$ | -0.256 | 0.798 | -0.026 |
| Passerines | $\log_{10}$ | Call vs Song – DF | 3.084 | 0.003 ** | 0.308 |

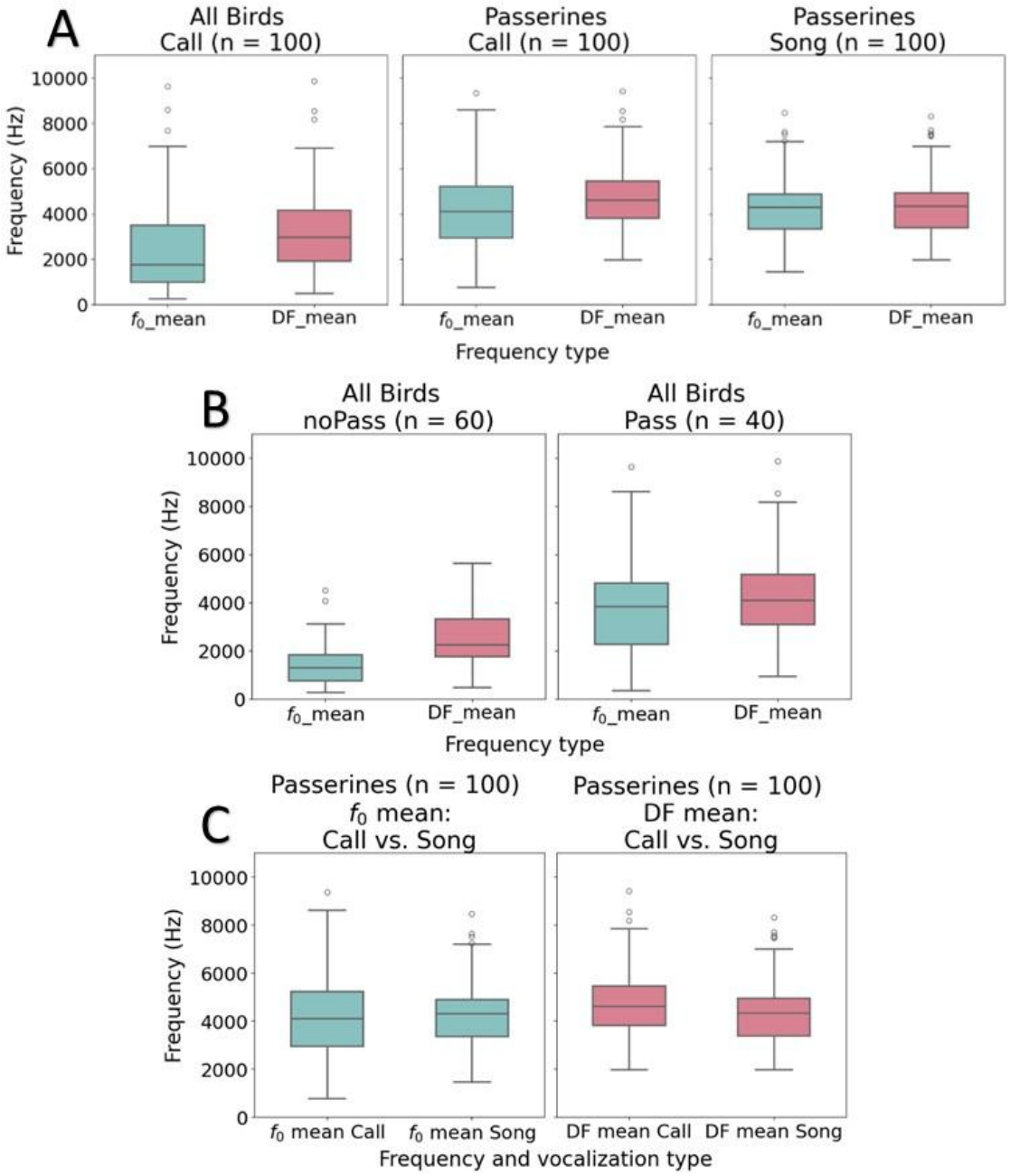


**Figure 6** Boxplots of $f_0$ and DF (A and B), illustrating t-test results of all datasets; A and B showing that DF was consistently higher than $f_0$. Boxplots of Passerines Call and Song (C) showing no difference in $f_0$ mean between calls and songs, but higher DF mean values for calls.

## 3.3 Linear Regression

### 3.3.1 $f_0$ mean vs. DF mean

Species-wise summary segments of each dataset were used for the linear regression analyses. Shapiro-Wilk tests indicated that the 'All Birds' dataset and its subsets ('Pass' and 'noPass') met the assumption of normality. For the 'Passerines' subsets, normality was not confirmed. However, diagnosis plots for the call subset showed no major deviations from the model assumptions. In the 'Passerines song' subset, three outliers (*Carduelis cannabina*, *Sitta krueperi*, *Ammomanes cincturus*, see table 5) were removed; although the Shapiro-Wilk test still indicated non-normality, diagnostic plots suggested that the model fit was acceptable.

**Table 5** Outliers removed from 'Passerines Song' subset to improve model assumption.

| **Oulier Species – Passerines Song** | | |
|---|---|---|
| **Species** | **$f_0$-mean (Hz)** | **DF-mean (Hz)** |
| *Carduelis cannabina* | 2774 | 5238 |
| *Sitta krueperi* | 1457 | 2921 |
| *Ammomanes cincturus* | 2341 | 4649 |

Linear regressions showed strong positive relationships between log-transformed $f_0$ and log-transformed DF across all datasets (see table 6). For the 'All Birds' dataset ($F_{1,98}$ = 166.4, $p < 0.001$; Fig. 7A), $f_0$ explained 63 % of the variance in DF. The 'noPass' subset showed a weaker relationship, explaining 42 % of the variance ($F_{1,58}$ = 42.3, $p < 0.001$; Fig. 7B), whereas the 'Pass' subset showed a stronger relationship, explaining 70 % ($F_{1,38}$ = 89.0, $p < 0.001$; Fig. 7B). Within the 'Passerines' dataset, $f_0$ explained 53 % of the variance in DF for the call subset ($F_{1,98}$ = 109.5, $p < 0.001$; Fig. 7A) and 95 % for the song subset ($F_{1,95}$ = 1965.0, $p < 0.001$; Fig. 7A).

**Table 6** Results of linear regression with DF as response and $f_0$ as predictor variable, both variables were $\log_{10}$ transformed.

| **$f_0$ mean vs. DF mean** | | | | | | | |
|---|---|---|---|---|---|---|---|
| **Model** | **n** | **$R^2$** | **F** | **β ($f_0$_log)** | **SE** | **t-value** | **p-value** |
| All Birds | 100 | 0.63 | 166.4 | 0.55 | 0.04 | 12.90 | <0.001 |
| All Birds - noPass | 60 | 0.42 | 42.3 | 0.52 | 0.08 | 6.50 | <0.001 |
| All Birds - Pass | 40 | 0.70 | 89.0 | 0.53 | 0.06 | 9.43 | <0.001 |
| Passerines Call | 100 | 0.53 | 109.5 | 0.51 | 0.05 | 10.46 | <0.001 |
| Passerines Song | 97 | 0.95 | 1965.0 | 0.98 | 0.02 | 44.33 | <0.001 |

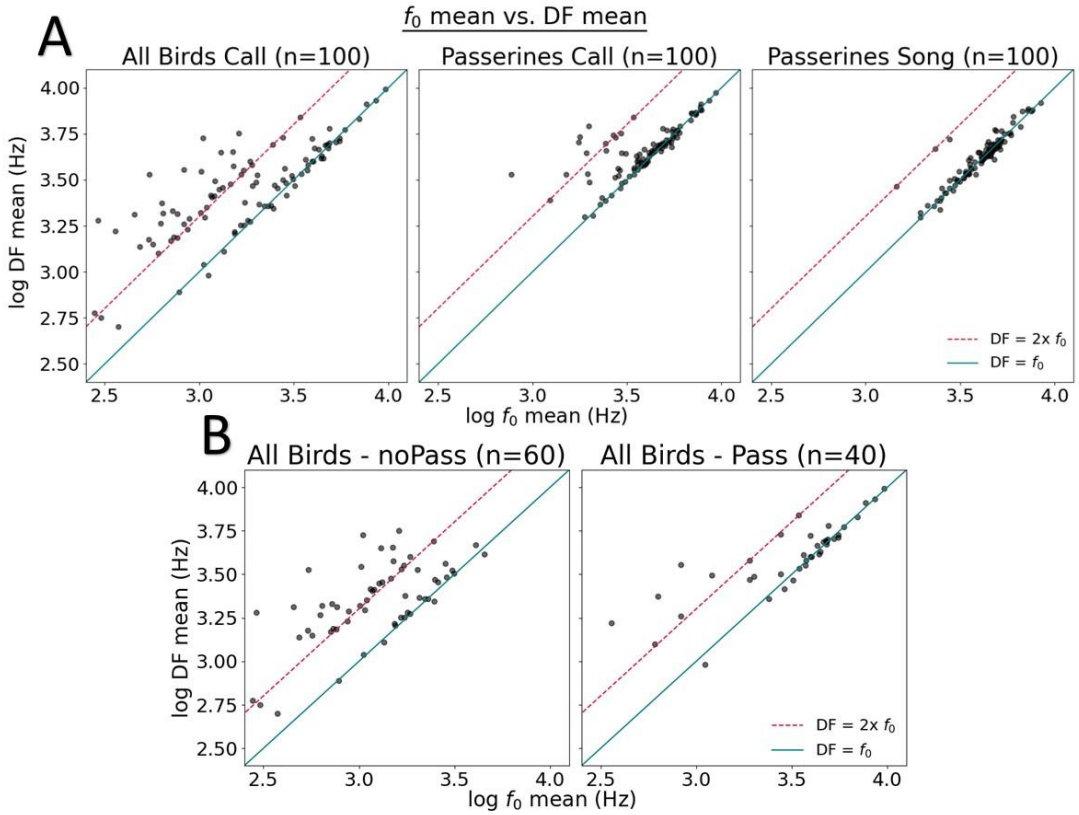


**Figure 7** Relationship between $f_0$ mean ($\log_{10}$) and DF mean ($\log_{10}$) of all datasets. Each datapoint represents one species. Solid line: DF = $f_0$, dashed line DF = $2f_0$;

### 3.3.2 Body mass vs. $f_0$ mean

Species-wise summary segments were also used to test for associations between body mass (log-transformed) and $f_0$ (log-transformed). The 'All Birds' dataset and its subsets met the assumption of normality. For the 'Passerines call' and 'Passerines song' subsets, normality was not confirmed, but after removal of two outliers (*Dumetella carolinensis*, *Ammomanes cincturus* for calls; *Sitta krueperi*, *Sylvia hortensis* for songs), the normality assumption was met. Linear regressions showed significant negative relationships between log-transformed body mass and $f_0$ across all datasets (Table 7). For the 'All Birds' dataset, body mass explained 49 % of the variance in $f_0$ ($F_{1,98} = 93.1$, $p < 0.001$; Fig. 8A). The relationship was weaker in the 'noPass' subset ($R^2 = 0.12$, $F_{1,58} = 8.0$, $p = 0.0065$; Fig. 8B), but stronger in the 'Pass' subset ($R^2 = 0.58$, $F_{1,38} = 53.1$, $p < 0.001$; Fig. 8B). Within the 'Passerines' dataset, body mass explained 10 % of the variance in $f_0$ in the call subset ($F_{1,96} = 10.3$, $p = 0.0018$; Fig. 8A) and 50 % in the song subset ($F_{1,96} = 96.3$, $p < 0.001$; Fig. 8A).

**Table 7** Results of linear regression with $f_0$ as response and body mass as predictor variable, both variables were $\log_{10}$ transformed.

| Body mass vs. $f_0$ mean | | | | | | | |
|---|---|---|---|---|---|---|---|
| **Model** | **n** | **$R^2$** | **F** | **β (mass log)** | **SE** | **t-value** | **p-value** |
| All Birds | 100 | 0.49 | 93.12 | -0.36 | 0.04 | -9.65 | <0.001 |
| All Birds - noPass | 60 | 0.12 | 7.98 | -0.20 | 0.07 | -2.82 | 0.0065 |
| All Birds - Pass | 40 | 0.58 | 53.07 | -0.53 | 0.07 | -7.29 | <0.001 |
| Passerines Call | 98 | 0.10 | 10.32 | -0.17 | 0.05 | -3.21 | 0.0018 |
| Passerines Song | 98 | 0.50 | 96.29 | -0.29 | 0.03 | -9.81 | <0.001 |

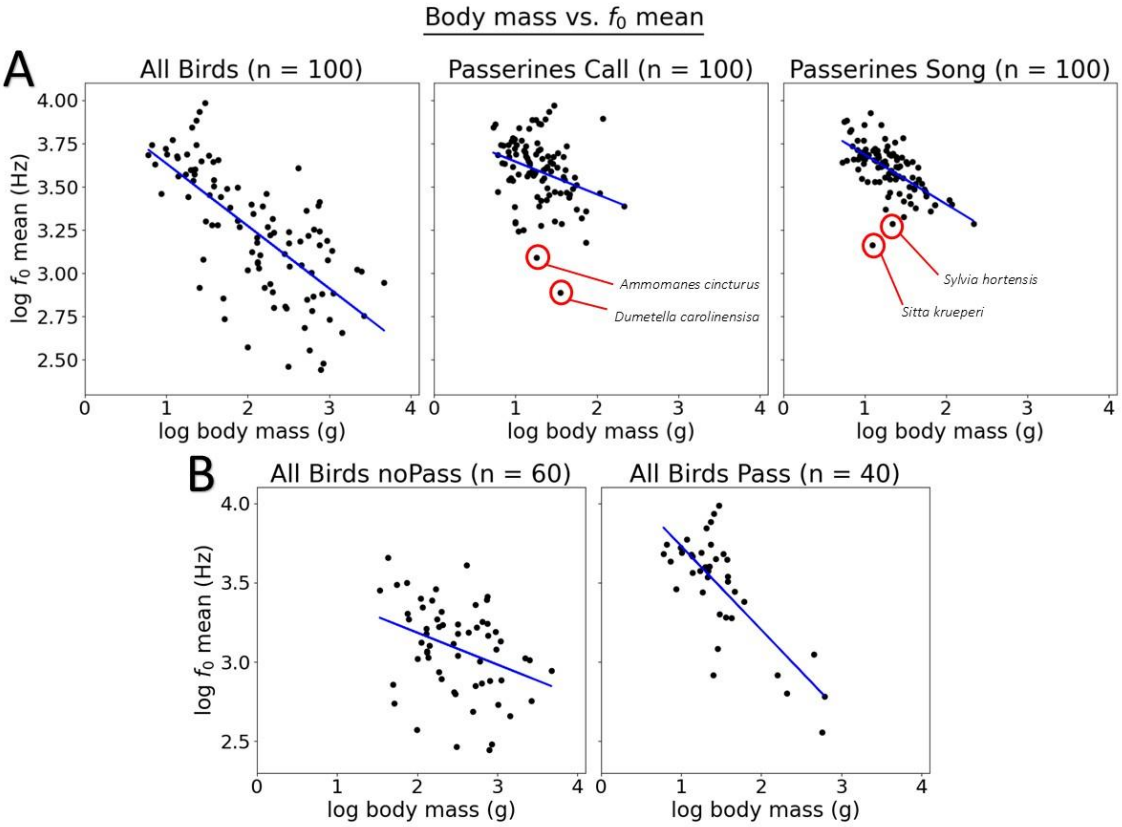


**Figure 8** Relationship between body mass ($\log_{10}$) and $f_0$ mean ($\log_{10}$). Each datapoint represents one species. The circled species show the removed outliers to improve model assumption. The blue line represents the fitted linear regression line.

## 3.4 Body size vs DF

Correlation analyses also showed strong negative associations between body mass and the other acoustic frequency measures in the 'All Birds' dataset (r = -0.73 for $f_0$-mean, r = -0.75 for DF-mean). This relationship was stronger in the 'Pass' subset (n = 40; r = -0.60 for $f_0$-mean, r = -0.59 for DF-mean), compared to the 'noPass' subset (n = 60, r = -0.36 for $f_0$-mean, r = -0.52 for DF-mean). Within Passerines, correlations were stronger

for songs (r = -0.65 for $f_0$-mean, r = -0.64 for DF-mean), than for calls (r = -0.35 for $f_0$-mean, r = -0.42 for DF-mean).

### 3.4.1 Other morphological Correlations

Beak parameters showed the strongest relationship with DF in the 'All Birds' dataset (r = -0.72 for beak length , r = -0.69 for beak depth, r = -0.61 for beak width), and its 'Pass' subset (r = -0.69 for beak length , r = -0.61 for beak depth, r = -0.64 for beak width). In the 'noPass' subset, correlations were moderate to weak (r = -0.37 for with beak length, r = -0.42 for beak depth, r = -0.26 for beak width). In the 'Passerines' dataset, correlations were moderate for the call subset (r = -0.43 length , r = -0.32 depth, r = -0.38 width), and moderate to strong in the song subset (r = -0.60 length , r = -0.48 depth, r = -0.48 width). A representative heatmap of the 'All Birds' dataset is shown in Figure 9; full correlation matrices for all datasets are provided in the Appendix.

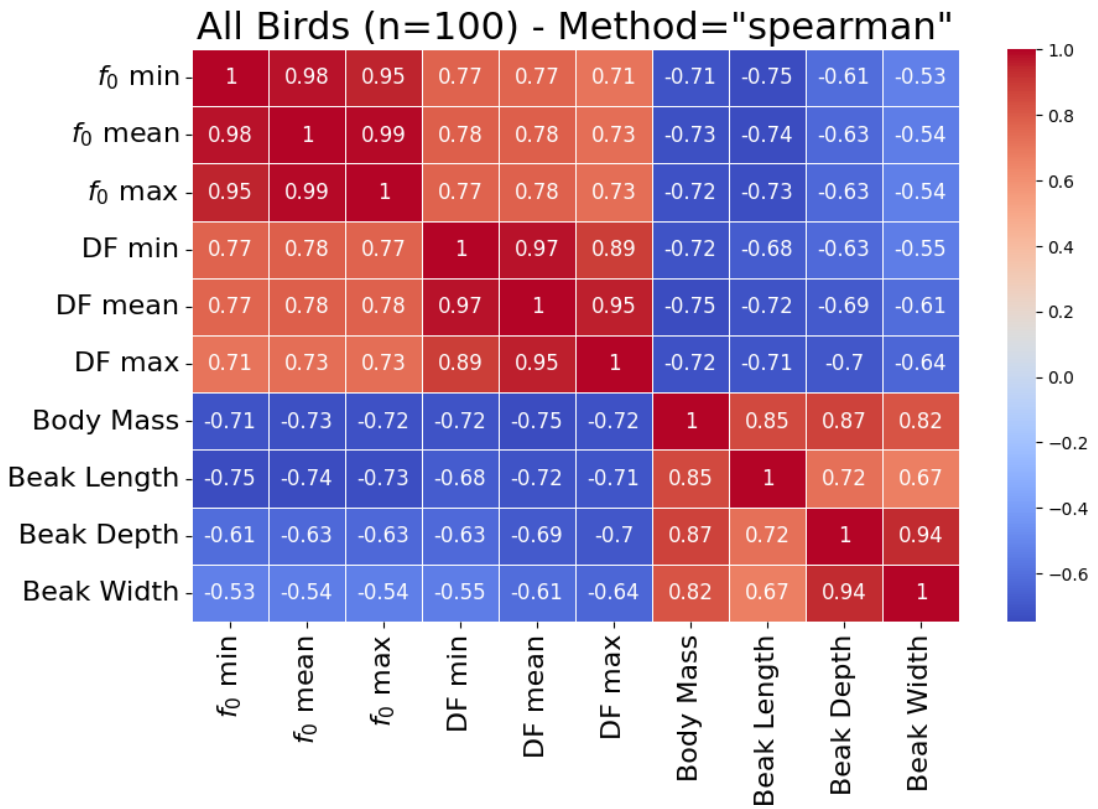


**Figure 9** Spearman rank correlation matrix for acoustic and morphological variables in the 'All Birds' dataset (n = 100). Warm colors indicate positive and cool colors negative correlations. Strong negative associations are evident between body mass and both $f_0$-mean and DF-mean ($p \approx -0.7$). DF also shows strong negative correlations with beak length and depth. These patterns suggest that larger species and those with longer or deeper beaks tend to produce lower dominant frequencies.

Partial correlations controlling for body mass confirmed that beak length showed a significant negative association with DF in the 'All Birds' dataset (p = 0.02), its 'Pass' subset (p = 0.004), and in the 'Passerines song' subset (p = 0.015). The 'Passerines call' subset showed a trend towards significance (p = 0.053). Beak depth was not significant in any dataset or subset, while beak width was significant only in the 'Pass' subset (p = 0.046). (see Table 8)

**Table 8** Partial correlation between DF and beak parameters (1: length, 2: depth, 3: width) corrected for body mass; ns = not significant; parameters are illustrated in the picture right of the tables adapted from Tobias et al (2022);

**A - DF vs. Beak Length (1) – corrected for body mass**

| Dataset | n | r | p-value | Sign. |
|---|---|---|---|---|
| All Birds | 100 | -0.231 | 0.02 | * |
| All Birds - noPass | 60 | -0.125 | 0.35 | ns |
| All Birds - Pass | 40 | -0.454 | 0.004 | ** |
| Passerines - Call | 100 | -0.194 | 0.053 | ns |
| Passerines - Song | 100 | -0.245 | 0.015 | * |

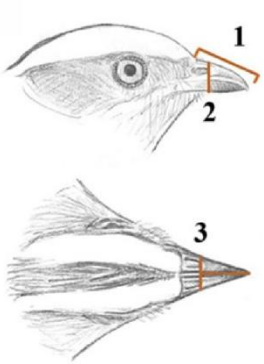


**B - DF vs. Beak Depth (2) – corrected for body mass**

| Dataset | n | r | p-value | Sign. |
|---|---|---|---|---|
| All Birds | 100 | -0.118 | 0.243 | ns |
| All Birds - noPass | 60 | 0.046 | 0.732 | ns |
| All Birds - Pass | 40 | -0.241 | 0.139 | ns |
| Passerines - Call | 100 | 0.010 | 0.920 | ns |
| Passerines - Song | 100 | 0.030 | 0.767 | ns |

**C - DF vs. Beak Width (3) – corrected for body mass**

| Dataset | n | r | p-value | Sign. |
|---|---|---|---|---|
| All Birds | 100 | -0.001 | 0.996 | ns |
| All Birds - noPass | 60 | 0.245 | 0.061 | ns |
| All Birds - Pass | 40 | -0.321 | 0.046 | * |
| Passerines - Call | 100 | -0.115 | 0.258 | ns |
| Passerines - Song | 100 | 0.005 | 0.957 | ns |

## 3.5 Phylogenetic Analyses

All phylogenetic analyses were performed on the 'All Birds' dataset (n = 77), pruned to fit the phylogenetic tree (see methods section 2.3.7).

### 3.5.1 Phylogenetic Signal – Blomberg's K and Pagel's λ

Phylogenetic signal analyses, all values stated in table 9 and visualized in figure 10, indicated significant phylogenetic structure for all acoustic and morphological traits in the 'All Birds' dataset (Blomberg's K: p = 0.001 for all traits). Across this dataset, K values ranged from 0.45 (DF mean) to 0.81 (beak width), indicating a moderate to strong phylogenetic signal. Pagel's λ values were consistently high (λ = 0.71–1.00). Among acoustic traits, $f_0$-mean exhibited a stronger phylogenetic signal (K = 0.65, λ = 0.83) than DF-mean (K = 0.45, λ = 0.71), whereas λ values showed high phylogenetic signal for morphological traits, with beak width and body mass reaching λ = 1.0. Thus, the acoustic traits measured here can retain phylogenetic signal levels comparable to morphological traits.

When Passerines and non-Passerines of the 'All Birds' dataset were analyzed separately, Passerines showed higher phylogenetic signal for both acoustic traits ($f_0$ mean: K = 0.85, λ = 0.77, p = 0.001; DF mean: K = 0.77, λ = 0.72, p = 0.001) compared to the noPass subset ($f_0$ mean: K = 0.33, λ = 0.47, p = 0.003; DF mean: K = 0.19, λ = 0.35, p = 0.127). This pattern suggest that acoustic frequency parameters are more strongly shaped by shared ancestry within Passerines, whereas DF in particular shows no significance in non-Passerines.

For morphological traits, Passerines showed particularly high K values for beak length (K = 1.40) and beak width (K = 1.90), with λ = 1.0 across all morphological variables, indicating strong phylogenetic conservatism. In contrast, non-Passerines showed lower K values for all beak measurements (K = 0.25-0.50) and lower λ for beak length and beak depth, and although most traits remained significant (p < 0.05), beak length (p = 0.013) and depth (p = 0.002) showed weaker signal strength, and beak width was the most strongly conserved trait (p = 0.001).

**Table 9** Phylogenetic signal: Blomberg's K and Pagel's λ values of the pruned 'All Birds' dataset and its subsets 'Pass' and 'noPass'. K_p indicates significance level. K = 1 represents signal expected under Brownian motion, K > 1 even higher than expected; λ = 0 means no, λ = 1 high signal;

| Phylogenetic Signal | | | | | | | | | |
|---|---|---|---|---|---|---|---|---|---|
| **Dataset:** | **All Birds** | | | **Pass** | | | **noPass** | | |
| **Trait** | **K_p** | **K** | **λ** | **K_p** | **K** | **λ** | **K_p** | **K** | **λ** |
| $f_0$ mean | 0.001 | 0.65 | 0.83 | 0.001 | 0.85 | 0.77 | 0.003 | 0.33 | 0.47 |
| DF mean | 0.001 | 0.45 | 0.71 | 0.001 | 0.77 | 0.72 | 0.127 | 0.19 | 0.35 |
| Body mass | 0.001 | 0.52 | 1.00 | 0.001 | 1.06 | 1.00 | 0.009 | 0.38 | 1.00 |
| Beak length | 0.001 | 0.52 | 0.87 | 0.001 | 1.40 | 1.00 | 0.013 | 0.25 | 0.25 |
| Beak depth | 0.001 | 0.60 | 0.96 | 0.001 | 1.73 | 1.00 | 0.002 | 0.38 | 0.80 |
| Beak width | 0.001 | 0.81 | 1.00 | 0.001 | 1.90 | 1.00 | 0.001 | 0.50 | 0.86 |

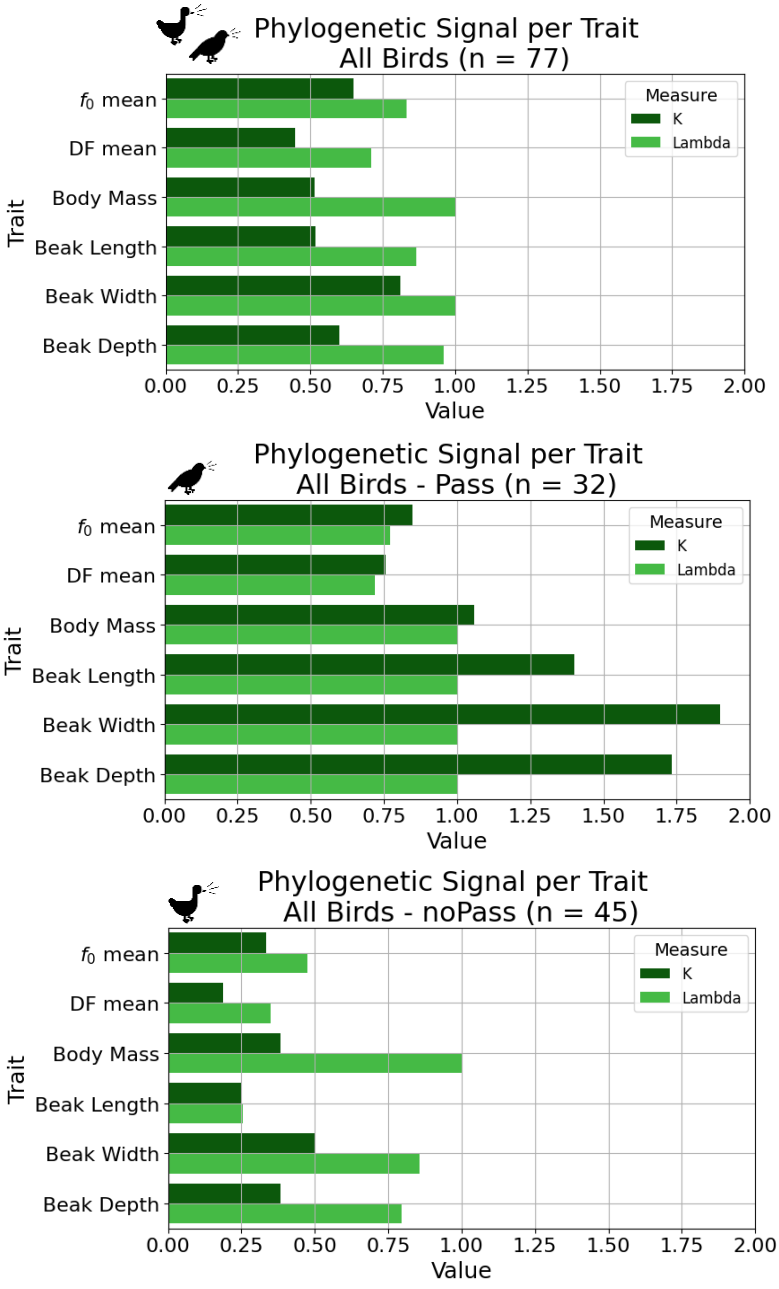


**Figure 10** Phylogenetic signal: Blomberg's K (dark green) and Pagel's λ (light green) of the 'All Birds' dataset and its subsets 'Pass' and 'noPass';

### 3.5.2 Phylogenetic Generalized Least Squares - PGLS

To select the most appropriate model for the PGLS analysis, multicollinearity was evaluated using variance inflation factor (VIF). The aim was to define one model explaining $f_0$ and another for DF. For the $f_0$ model, only body mass was used as a predictor. For the DF model, including $f_0$, body mass, and all three beak parameters resulted in VIF values exceeding common thresholds (VIF > 5) for the 'All Birds' pruned dataset, indicating problematic collinearity. Stepwise model reduction lowered the VIF values.

A relative importance analysis confirmed that $f_0$ and beak length together explained more than 70% of the variance in DF, with the remaining predictors contributing less than 1% additional variance. This justified the choice of the final, reduced DF model.

The two final models:

- $f_0$ (log) ~ body mass (log)
- DF (log) ~ $f_0$ (log) + beak length

The same models were used for the 'Pass' (n = 32) and 'noPass' (n = 45) subsets. The VIF-values showed the lowest collinearity effect for the reduced model here as well. And the relative importance check showed ~75% variance explanation in the 'Pass' subset, when using the model with $f_0$ (log) and beak length, with <5% additional variance explained by adding all parameters. In the 'noPass' subset, ~58% of variance is explained by this model, with <1% additional explanation by adding more parameters.

Shapiro-Wilk test showed for the 'All Birds' dataset normal distribution for the $f_0$ model with both parameters log-transformed, and for the DF model with beak length untransformed. For the 'Pass' and 'noPass' subset a log-transformation of beak length improved the Akaike Information Criterion (AIC), while normality was confirmed for log-transformed and untransformed beak length.

For the $f_0$ model, performed on the 'All Birds' dataset, body mass showed a significant negative effect on $f_0$ ($t = -2.53$, $p = 0.014$), indicating that larger-bodied species tend to have lower $f_0$, even after accounting for phylogeny (Fig. 11A).
For the DF model, both predictors had significant effects on DF in the 'All Birds' dataset: $f_0$ was positively associated ($t = 3.08$, $p = 0.003$; Fig. 11A), whereas beak length showed a negative association ($t = -3.28$, $p = 0.002$; Fig. 11A) with DF.

Passerines from the 'All Birds' dataset, showed no significant effect of body mass on $f_0$ (t = -1.10, p = 0.28) after accounting for phylogeny, whereas in non-Passerines body mass did have a significant effect (t = -2.21, p = 0.03, Fig. 11B). For the DF model, $f_0$ showed no significant effect on DF (t = 0.12, p = 0.91), but beak length did (t = -4.53, p = 0.0001, Fig. 11B). In the non-Passerines subset $f_0$ showed a significant effect on DF (t = 2.71, p = 0.0097, Fig. 11B), but there was no significance for beak length (t = -1.66, p = 0.10).

**Table 10** PGLS-results for the two models performed on the 'All Birds' dataset and its subset 'Pass' and noPass'

| **Dataset** | **n** | **$f_0$ ~ Body mass (BM)** | **DF ~ $f_0$ + Beak length (BL)** |
|---|---|---|---|
| **All Birds** | 77 | BM: t = 2.53, p = 0.014 * | $f_0$: t = 3.08, p = 0.003 **<br>BL: t = -3.28, p = 0.002 ** |
| **All Birds Pass** | 32 | BM: t = -1.10, p = 0.28 | $f_0$: t = 0.12, p = 0.91<br>BL: t = -4.53, p = 0.0001 *** |
| **All Birds noPass** | 45 | BM: t = -2.21, p = 0.03 * | $f_0$: t = 2.71, p = 0.0097 **<br>BL: t = -1.66, p = 0.10 |

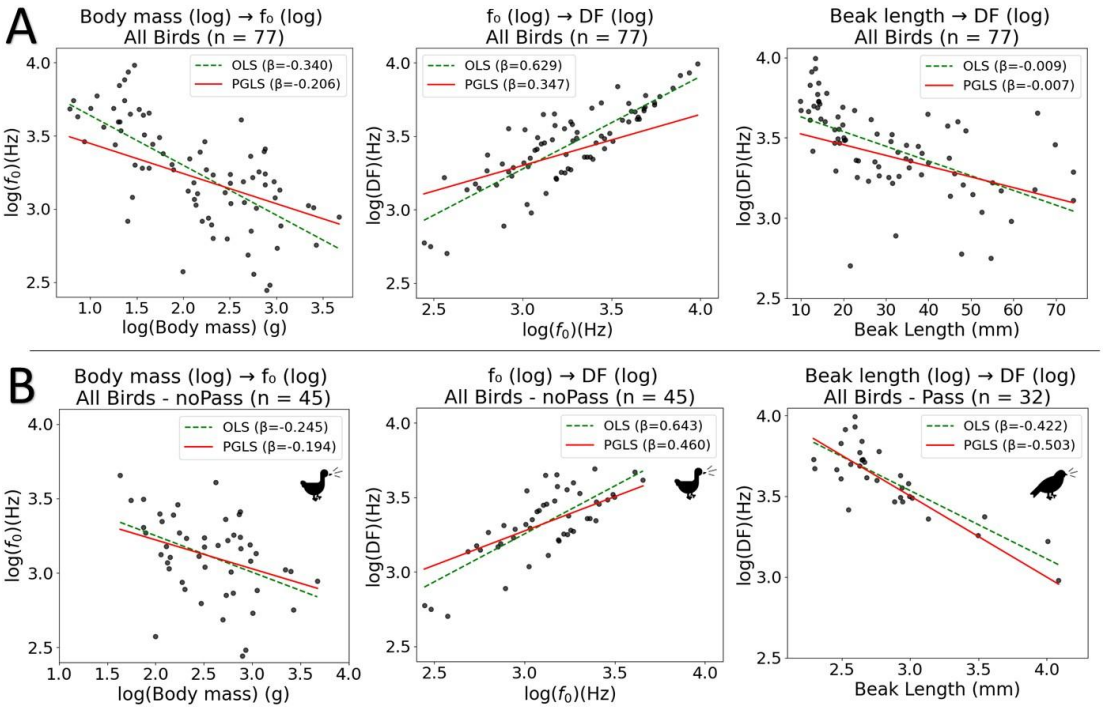


**Figure 11** OLS vs PGLS comparison of all significant outcomes of the PGLS models performed on the 'All Birds' data (A) and its subsets (B). The dashed green line represents the fitted slope of an ordinary least squares model, the red line the adapted slope corrected for phylogeny.

# 4. Discussion

This study investigated the relationship between fundamental frequency $f_0$ and the dominant frequency DF in a broad comparative dataset of avian vocalizations, combining acoustic analyses with morphological predictors and phylogenetic controls. The results show that there is a close relationship between both acoustic parameters, especially in Passerines songs, but that they are not identical. The variance in both frequency measures is partly explained by morphological and phylogenetic parameters.

## 4.1 $f_0$ vs. DF

### 4.1.1 Non-equivalence of $f_0$ and DF

DF was significantly higher than $f_0$ across all datasets, often ($f_0$-range) aligning with an upper harmonic, typically the second harmonic ($2f_0$). This demonstrates that the two parameters are not interchangeable and highlights the need to distinguish between source-related ($f_0$) and filter-related (DF) aspects of sound production, as previously reported in anurans (Gingras et al., 2013). At the same time, linear regression showed significant positive relationships between $f_0$ and DF across all datasets. In the 'All Birds' dataset, DF corresponded to $f_0$ in only about 50% of individual segments, while in the remainder it corresponded to $2f_0$ or higher harmonics. This means that uncritical use of DF as a proxy for $f_0$ would systematically bias results. The complexity of this relationship is further illustrated by occasional cases where DF aligned with the third harmonic ($3f_0$) or some other frequency.

In contrast, Passerine songs consistently exhibited a close match between DF and $f_0$. In around 95% of the individual segments, DF equalled $f_0$. Although statistical test still indicated significant difference between the two measures, only three species (*Carduelis cannabina, Sitta krueperi, Ammomanes cincturus*) showed a clear deviation from the 1:1 ratio.

Together, these results indicate that DF can only serve as a reliable proxy for $f_0$ under specific conditions, particularly in tonal song vocalizations of Passerines.

### 4.1.2 Song vs. Calls: Evidence for Active Vocal Tract Tuning

The tight coupling of $f_0$ and DF in songs is consistent with active vocal tract tuning to $f_0$, which enhances tonal clarity and suppresses harmonics (Riede et al., 2006). The nearly

perfect linear relationship between $f_0$ and DF in Passerines songs ($R^2$ = 0.95, after removing three outliers), when contrasted with the other vocalizations analyzed here, supports the hypothesis that songbirds actively use their vocal tract to amplify $f_0$ via formant tuning. Calls, in contrast, showed a weaker correspondence between $f_0$ and DF ($R^2$ = 0.53), with elevated DF values, often near $2f_0$. This suggests less effort on tuning and a possible functional shift towards maximizing transmission efficiency (Friis et al., 2022).

Songs are typically associated with territory defence and mate choice, where signal quality is often under strong sexual selection (Podos et al., 2004). Producing songs in which DF emphasizes $f_0$ may therefore enhance attractiveness to potential mates or intimidate rivals by amplifying allometric cues. According to the 'acoustic allometry', bigger animals can produce lower $f_0$'s (e.g., Martin et al., 2011), this can serve as an information about the size of the sender and potentially improve the senders success in competitive situations. Therefore, active tuning of the vocal tract so that DF amplifies $f_0$ may thus support this size-related signal.

To further investigate these relationships, traits that potentially represent source characteristics (body mass) and filter characteristics (beak morphology) were taken into account.

## 4.2 Source vs. Filter: Body Size and Beak Morphology

Regression analyses confirmed across all datasets that $f_0$ scales negatively with body size, which aligns with the 'acoustic allometry' thesis. The strongest relationships were observed in the 'All Birds' dataset ($R^2$ = 0.49), its Passerines subset ($R^2$ = 0.58), and in the Passerine song dataset ($R^2$ = 0.50). The family-level 'All Birds' dataset provided a balanced representation of size diversity, whereas the Passerine call and song subsets were less balanced in terms of relatedness. Nevertheless, the regressions indicated a closer relationship between $f_0$ and body size in the song subset compared to the call subset. The correlation matrices support this result between $f_0$ mean and body mass (song: r = -0.65, call: r = -0.35). Although there was no significant difference between $f_0$ mean in calls and songs in Passerines, there was a stronger relationship according to linear regression.

A relationship with DF to potential filter components among all three beak parameters (length, depth, width) was noticeable for beak length. Partial correlations controlling for

body mass, showed that beak length significantly predicted DF in Passerine song and in the family-level Passerines subset. This suggests that beak length acts as a filter parameter during vocal tract tuning. This result aligns with previous studies demonstrating that beak morphology can constrain and shape acoustic frequencies (Huber & Podos, 2006). Of the other two beak measurements, only beak width showed a significant effect in the 'All Birds – Pass' subset, while beak depth showed no significance, suggesting that beak length plays the dominant role in shaping resonance frequencies.

## 4.3 Phylogenetic Structure

Phylogenetic analyses were performed on the 'All Birds' dataset and on its Passerine ('Pass') and non-Passerine ('noPass') subsets. Phylogenetic signal was present for all acoustic and morphological traits in the 'All Birds' dataset. When separated, non-Passerines showed no significant signal for DF ($K = 0.19$, $p = 0.127$, $\lambda = 0.35$), whereas Passerines displayed stronger phylogenetic signal for both acoustic and morphological traits. This discrepancy could reflect differences in selective pressure. As mentioned before, songs are subject to strong sexual selection (Podos et al., 2004), which may constrain DF to track $f_0$ and thereby establish lineage-specific frequency ranges. Non-Passerines might be constrained rather by environmental influences, like for example habitat structure or ambient noise. Further investigation is needed to disentangle the roles of selection and sampling artefacts.

Notably, beak traits in Passerines were even more phylogenetically conserved than expected under a Brownian motion model (e.g. beak width: $K = 1.90$, $\lambda = 1.0$). These results suggest that vocal frequency parameters are phylogenetically more conserved within Passerines, consistent with findings of Friis et al. (2022), who also reported stronger phylogenetic signal for acoustic traits in songbirds.

### 4.3.1 Source-Filter Perspective

In the 'All Birds' dataset, all predictors had significant effects on the acoustic response variables $f_0$ and DF. A closer look into the subsets, however, showed contrasting patterns between Passerines and non-Passerines. In Passerines, variance in $f_0$ was mostly explained by phylogenetic relatedness rather than by body mass. Furthermore, DF was strongly influenced by beak length, while the effect of $f_0$ was almost entirely accounted for by relatedness. In non-Passerines, the pattern was reversed: body mass remained a

significant predictor of $f_0$ even after phylogenetic correction, and $f_0$ significantly predicted DF, but beak length showed no detectable effect.

In the Passerines subset, body mass ranged from 6 to 570 g (mean ≈ 65 g), whereas in the non-Passerines it spanned from 43 to 4,729 g (mean ≈ 663 g). Beak length varied between 9.9 and 59.5 mm in Passerines (mean ≈ 19 mm) and 17.9 to 74.1 mm in non-Passerines (mean ≈ 39 mm). Thus, non-Passerines not only cover a broader absolute range of body sizes but are also on average considerably larger, which may account for the stronger scaling of $f_0$ with body mass. By contrast, while on average non-Passerines were about ten times heavier (≈ 663 g vs. ≈ 65 g), beak length was only about twice as large (≈ 39 mm vs. ≈ 19 mm). This suggests that the stronger predictive role of beak length in Passerines reflects functional differences in vocal tract filtering rather than simply differences in morphological variation.

These findings support the view that Passerines, in contrast to non-Passerines, actively use beak morphology to filter the resonance frequencies in the vocal tract.

The phylogenetic analyses highlight the importance of including phylogeny in comparative analysis to avoid pseudoreplication and overestimating effects that may partly be explained by relatedness (Felsenstein, 1985).

## 4.4 Limitations and Future Directions

Although this study included 100 species across 20 families, the dataset was limited to European birds, and some orders remain underrepresented. Additional data, particularly from non-Passerines, would help to clarify whether the low phylogenetic signal of DF is a general pattern or a sampling artifact.

Future research could also address the functional implications of the many cases where DF is higher than $f_0$. Testing whether this is based on carrying communicative information or has adaptive value (e.g. better signal transmission), would provide important insights into the evolution of bird vocalizations.

Finally, a comparison between Oscines and Suboscines – representing vocally learnt versus innate vocalizations – could help to understand the role of vocal learning in shaping source-filter interactions. Complementary phylogenetic analyses concerning the

difference between call and song, could deepen the understanding of the filter effect we observed in songbirds vocalizations.

## 4.5 Conclusion

This study shows that DF can be a reliable proxy for $f_0$ in Passerine songs, but that this 1:1 relationship fails across all birds. $f_0$ and DF are complementary, but not interchangeable parameters. Using DF as a surrogate for $f_0$ risks systematic bias towards higher frequencies, especially in calls. In taxonomically broad datasets, direct extraction of $f_0$ (e.g., via autocorrelation) should therefore be preferred whenever possible, and interpretations based solely on DF must be made with caution.

Morphological traits and phylogenetic relatedness explain a substantial portion of the variation in acoustic parameters, underscoring the need to account for those factors in comparative bioacoustics research.

These findings have methodological implications for studies that use DF as a substitute for $f_0$ and contribute to a more nuanced understanding of the evolution of avian vocal frequency parameters.

# 5. References


Blomberg, S. P., Garland JR., T., & Ives, A. R. (2003). Testing for Phylogenetic Signal in Comparative Data: Behavioral Traits Are More Labile. *Evolution*, *57*(4), 717–745. https://doi.org/10.1111/j.0014-3820.2003.tb00285.x

Boersma, P. (1996, 2001–2003,2022–2024). *Sound: To Pitch (ac)...* https://www.fon.hum.uva.nl/praat/manual/Sound__To_Pitch__ac____.html

Catchpole, C. (with Slater, P. J. B.). (2008). *Bird song: Biological themes and variations* (Second edition.). Cambridge University Press,. https://doi.org/10.1017/CBO9780511754791

Demery, A.-J. C., Burns, K. J., & Mason, N. A. (2021). Bill size, bill shape, and body size constrain bird song evolution on a macroevolutionary scale. *Ornithology*, *138*(2), ukab011. https://doi.org/10.1093/ornithology/ukab011

Elemans, C., Larsen, O., Hoffmann, M., & Van Leeuwen, J. (2003). Quantitative modelling of the biomechanics of the avian syrinx. *Animal Biology*, *53*(2), 183–193. https://doi.org/10.1163/157075603769700377

Elemans, C. P. (2014). The singer and the song: The neuromechanics of avian sound production. *Current Opinion in Neurobiology*, *28*, 172–178. https://doi.org/10.1016/j.conb.2014.07.022

Elemans, C. P. H., Rasmussen, J. H., Herbst, C. T., Düring, D. N., Zollinger, S. A., Brumm, H., Srivastava, K., Svane, N., Ding, M., Larsen, O. N., Sober, S. J., & Švec, J. G. (2015). Universal mechanisms of sound production and control in birds and mammals. *Nature Communications*, *6*(1), 8978. https://doi.org/10.1038/ncomms9978

Felsenstein, J. (1985). Phylogenies and the Comparative Method. *The American Naturalist*, *125*(1), 1–15. https://doi.org/10.1086/284325

Fitch, W. T. (1999). Acoustic exaggeration of size in birds via tracheal elongation: Comparative and theoretical analyses. *Journal of Zoology*, *248*(1), 31–48. https://doi.org/10.1111/j.1469-7998.1999.tb01020.x

Friis, J. I., Sabino, J., Santos, P., Dabelsteen, T., & Cardoso, G. C. (2022). Ecological adaptation and birdsong: How body and bill sizes affect passerine sound frequencies. *Behavioral Ecology*, *33*(4), 798–806.

Gingras, B., Boeckle, M., Herbst, C. T., & Fitch, W. T. (2013). Call acoustics reflect body size across four clades of anurans. *Journal of Zoology*, *289*(2), 143–150. https://doi.org/10.1111/j.1469-7998.2012.00973.x

Grömping, U. (2006). Relative Importance for Linear Regression in *R*: The Package **relaimpo**. *Journal of Statistical Software*, *17*(1). https://doi.org/10.18637/jss.v017.i01

Hackett, S. J., Kimball, R. T., Reddy, S., Bowie, R. C. K., Braun, E. L., Braun, M. J., Chojnowski, J. L., Cox, W. A., Han, K.-L., Harshman, J., Huddleston, C. J., Marks, B. D., Miglia, K. J., Moore, W. S., Sheldon, F. H., Steadman, D. W., Witt, C. C., & Yuri, T. (2008). A Phylogenomic Study of Birds Reveals Their Evolutionary History. *Science*, *320*(5884), 1763–1768. https://doi.org/10.1126/science.1157704

Herbst, C. T., Elemans, C. P. H., Tokuda, I. T., Chatziioannou, V., & Švec, J. G. (2025). Dynamic System Coupling in Voice Production. *Journal of Voice*, *39*(2), 304–316. https://doi.org/10.1016/j.jvoice.2022.10.004

Hoese, W. J., Podos, J., Boetticher, N. C., & Nowicki, S. (2000). Vocal Tract Function in Birdsong Production: Experimental Manipulation of Beak Movements. *Journal of Experimental Biology*, *203*(12), 1845–1855. https://doi.org/10.1242/jeb.203.12.1845

Hopp, S. L., Owren, M. J., & Evans, C. S. (Eds). (1998). *Animal Acoustic Communication: Sound Analysis and Research Methods*. Springer. https://doi.org/10.1007/978-3-642-76220-8

Huber, S. K., & Podos, J. (2006). Beak morphology and song features covary in a population of Darwin's finches (Geospiza fortis): Beak Morphology and Vocal Production. *Biological Journal of the Linnean Society*, *88*(3), 489–498. https://doi.org/10.1111/j.1095-8312.2006.00638.x

Hunter, J. D. (2007). Matplotlib: A 2D Graphics Environment. *Computing in Science & Engineering*, *9*(3), 90–95. https://doi.org/10.1109/MCSE.2007.55

Jadoul, Y., Thompson, B., & De Boer, B. (2018). Introducing Parselmouth: A Python interface to Praat. *Journal of Phonetics*, *71*, 1–15. https://doi.org/10.1016/j.wocn.2018.07.001

Jetz, W., Thomas, G. H., Joy, J. B., Hartmann, K., & Mooers, A. O. (2012). The global diversity of birds in space and time. *Nature*, *491*(7424), 444–448. https://doi.org/10.1038/nature11631

Marler, P. (2004). Bird calls: A cornucopia for communication. In *Nature's Music* (pp. 132–177). Elsevier. https://doi.org/10.1016/B978-012473070-0/50008-6

Martin, J. P., Doucet, S. M., Knox, R. C., & Mennill, D. J. (2011). Body size correlates negatively with the frequency of distress calls and songs of Neotropical birds: *Body Size and Frequency of Calls and Songs*. *Journal of Field Ornithology*, *82*(3), 259–268. https://doi.org/10.1111/j.1557-9263.2011.00329.x

McFee, B., Raffel, C., Liang, D., Ellis, D., McVicar, M., Battenberg, E., & Nieto, O. (2015). *librosa: Audio and Music Signal Analysis in Python*. 18–24. https://doi.org/10.25080/Majora-7b98e3ed-003

McKinney, W. (2010). *Data Structures for Statistical Computing in Python*. 56–61. https://doi.org/10.25080/Majora-92bf1922-00a

Nowicki, S. (1987). Vocal tract resonances in oscine bird sound production: Evidence from birdsongs in a helium atmosphere. *Nature*, *325*(6099), 53–55.

Pagel, M. (1999). The Maximum Likelihood Approach to Reconstructing Ancestral Character States of Discrete Characters on Phylogenies. *Systematic Biology*, *48*(3), 612–622. https://doi.org/10.1080/106351599260184

Paradis, E., & Schliep, K. (2019). ape 5.0: An environment for modern phylogenetics and evolutionary analyses in R. *Bioinformatics*, *35*(3), 526–528. https://doi.org/10.1093/bioinformatics/bty633

Patterson, D. K., & Pepperberg, I. M. (1994). A comparative study of human and parrot phonation: Acoustic and articulatory correlates of vowels. *The Journal of the Acoustical Society of America*, *96*(2), 634–648. https://doi.org/10.1121/1.410303

Pearse, W. D., Davies, T. J., & Wolkovich, E. M. (2025). How to Define, Use, and Interpret Pagel's \ łambda \ (Lambda) in Ecology and Evolution. *Global Ecology and Biogeography*, *34*(4), e70012. https://doi.org/10.1111/geb.70012

Pennell, M. W., Eastman, J. M., Slater, G. J., Brown, J. W., Uyeda, J. C., FitzJohn, R. G., Alfaro, M. E., & Harmon, L. J. (2014). geiger v2.0: An expanded suite of methods for fitting macroevolutionary models to phylogenetic trees. *Bioinformatics*, *30*(15), 2216–2218. https://doi.org/10.1093/bioinformatics/btu181

Podos, J., Huber, S. K., & Taft, B. (2004). Bird Song: The Interface of Evolution and Mechanism. *Annual Review of Ecology, Evolution, and Systematics*, *35*(1), 55–87. https://doi.org/10.1146/annurev.ecolsys.35.021103.105719

Revell, L. J. (2024). phytools 2.0: An updated R ecosystem for phylogenetic comparative methods (and other things). *PeerJ*, *12*, e16505. https://doi.org/10.7717/peerj.16505

Revell, L. J., & Harmon, L. J. (2022). *Phylogenetic Comparative Methods in R*. Princeton University Press.

Riede, T., Suthers, R. A., Fletcher, N. H., & Blevins, W. E. (2006). Songbirds tune their vocal tract to the fundamental frequency of their song. *Proceedings of the National Academy of Sciences*, *103*(14), 5543–5548. https://doi.org/10.1073/pnas.0601262103

Sainburg, T. (2025). *Timsainb/noisereduce* [Jupyter Notebook]. https://github.com/timsainb/noisereduce (Original work published 2019)

Schulze, A. (Ed.). (2003). *Die Vogelstimmen Europas, Nordafrikas und Vorderasien: 2.817 Tonaufnahmen von 819 Vogelarten*. Ample Edition.

Seabold, S., & Perktold, J. (2010). *Statsmodels: Econometric and Statistical Modeling with Python*. 92–96. https://doi.org/10.25080/Majora-92bf1922-011

Suthers, R. A. (1990). Contributions to birdsong from the left and right sides of the intact syrinx. *Nature*, *347*(6292), 473–477. https://doi.org/10.1038/347473a0

Suthers, R. A. (2004). How birds sing and why it matters. In *Nature's Music* (pp. 272–295). Elsevier. https://doi.org/10.1016/B978-012473070-0/50012-8

Tobias, J. A., Sheard, C., Pigot, A. L., Devenish, A. J. M., Yang, J., Sayol, F., Neate-Clegg, M. H. C., Alioravainen, N., Weeks, T. L., Barber, R. A., Walkden, P. A., MacGregor, H. E. A., Jones, S. E. I., Vincent, C., Phillips, A. G., Marples, N. M., Montaño-Centellas, F. A., Leandro-Silva, V., Claramunt, S., … Schleuning, M. (2022). AVONET: Morphological, ecological and geographical data for all birds. *Ecology Letters*, *25*(3), 581–597. https://doi.org/10.1111/ele.13898

Vallat, R. (2018). Pingouin: Statistics in Python. *Journal of Open Source Software*, *3*(31), 1026. https://doi.org/10.21105/joss.01026

Virtanen, P., Gommers, R., Oliphant, T. E., Haberland, M., Reddy, T., Cournapeau, D., Burovski, E., Peterson, P., Weckesser, W., Bright, J., Van Der Walt, S. J., Brett, M., Wilson, J., Millman, K. J., Mayorov, N., Nelson, A. R. J., Jones, E., Kern, R., Larson, E., … Vázquez-Baeza, Y. (2020). SciPy 1.0: Fundamental algorithms for scientific computing in Python. *Nature Methods*, *17*(3), 261–272. https://doi.org/10.1038/s41592-019-0686-2

Waskom, M. (2023) „mwaskom/seaborn: v0.13.2 (September 2023)“. Zenodo. doi: 10.5281/zenodo.8393472.

# 6. Supplementary Material

## I. Additional heatmap matrices:

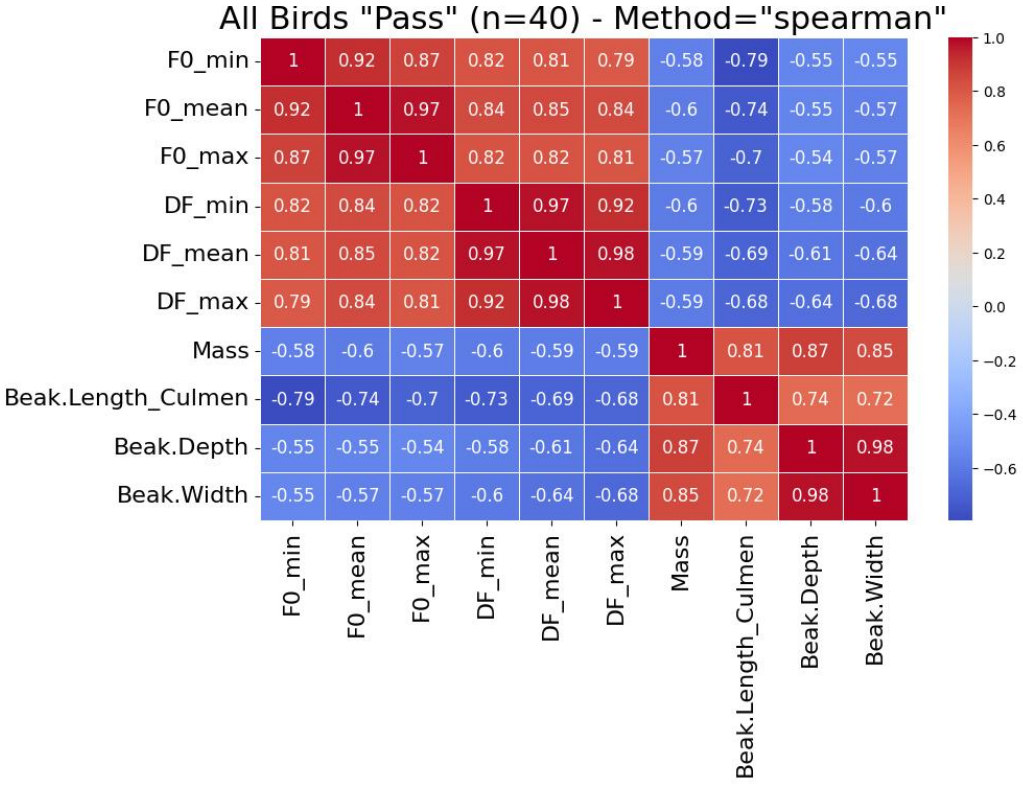


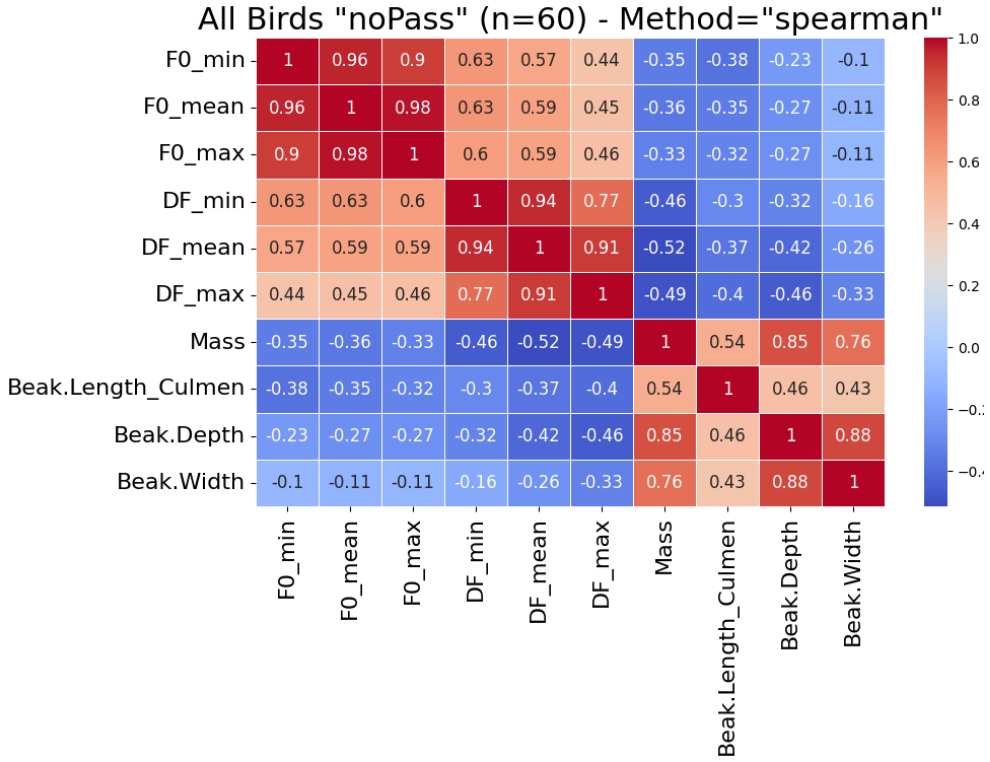

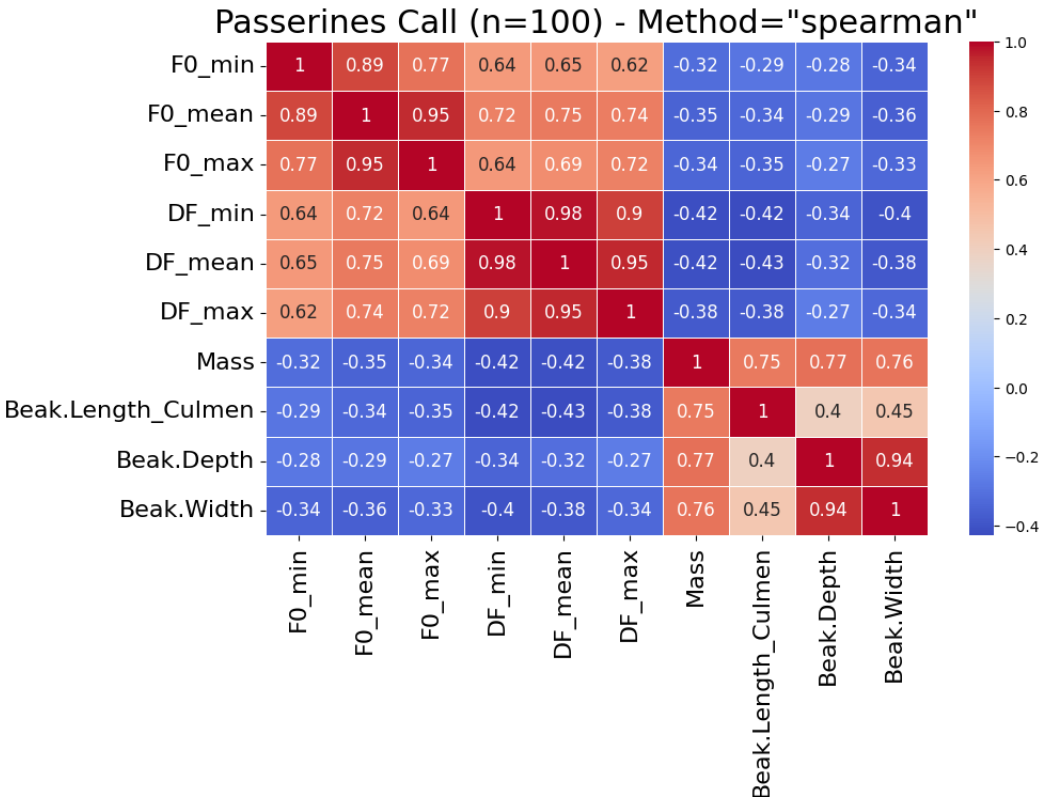
Passerines Call (n=100) - Method="spearman"
F0_min 1 0.89 0.77 0.64 0.65 0.62 -0.32 -0.29 -0.28 -0.34
F0_mean 0.89 1 0.95 0.72 0.75 0.74 -0.35 -0.34 -0.29 -0.36
F0_max 0.77 0.95 1 0.64 0.69 0.72 -0.34 -0.35 -0.27 -0.33
DF_min 0.64 0.72 0.64 1 0.98 0.9 -0.42 -0.42 -0.34 -0.4
DF_mean 0.65 0.75 0.69 0.98 1 0.95 -0.42 -0.43 -0.32 -0.38
DF_max 0.62 0.74 0.72 0.9 0.95 1 -0.38 -0.38 -0.27 -0.34
Mass -0.32 -0.35 -0.34 -0.42 -0.42 -0.38 1 0.75 0.77 0.76
Beak.Length_Culmen -0.29 -0.34 -0.35 -0.42 -0.43 -0.38 0.75 1 0.4 0.45
Beak.Depth -0.28 -0.29 -0.27 -0.34 -0.32 -0.27 0.77 0.4 1 0.94
Beak.Width -0.34 -0.36 -0.33 -0.4 -0.38 -0.34 0.76 0.45 0.94 1
F0_min F0_mean F0_max DF_min DF_mean DF_max Mass Beak.Length_Culmen Beak.Depth Beak.Width
1.0 0.8 0.6 0.4 0.2 0.0 −0.2 −0.4

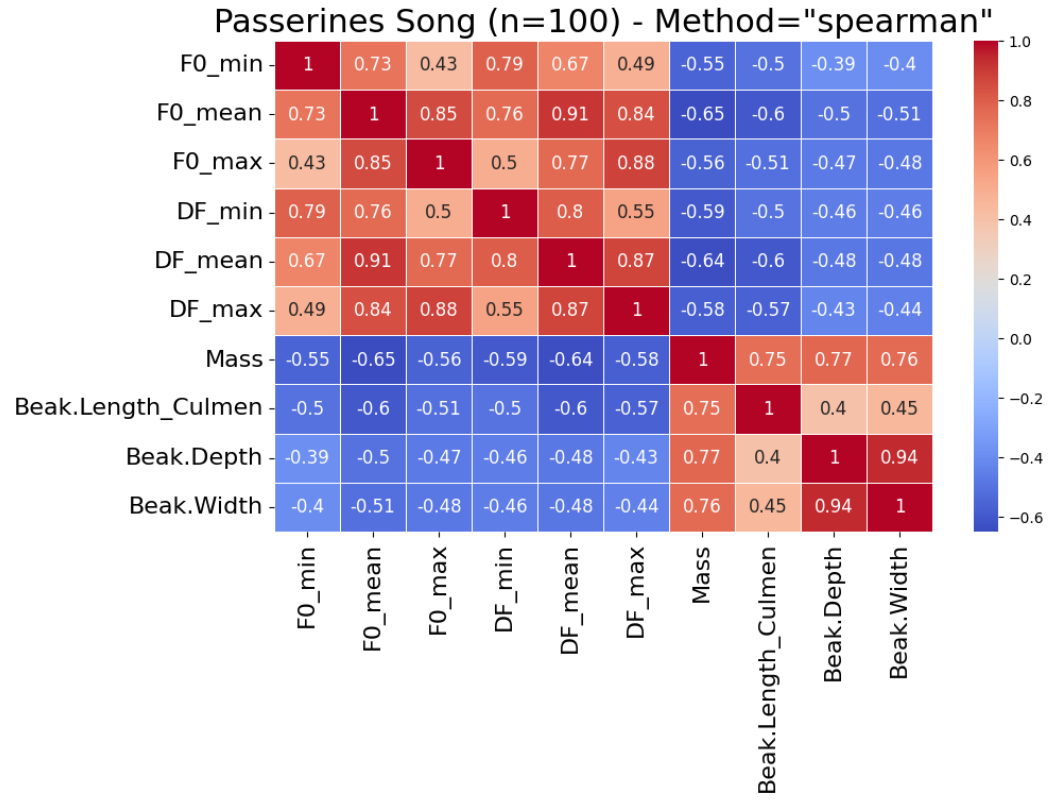
Passerines Song (n=100) - Method="spearman"
F0_min 1 0.73 0.43 0.79 0.67 0.49 -0.55 -0.5 -0.39 -0.4
F0_mean 0.73 1 0.85 0.76 0.91 0.84 -0.65 -0.6 -0.5 -0.51
F0_max 0.43 0.85 1 0.5 0.77 0.88 -0.56 -0.51 -0.47 -0.48
DF_min 0.79 0.76 0.5 1 0.8 0.55 -0.59 -0.5 -0.46 -0.46
DF_mean 0.67 0.91 0.77 0.8 1 0.87 -0.64 -0.6 -0.48 -0.48
DF_max 0.49 0.84 0.88 0.55 0.87 1 -0.58 -0.57 -0.43 -0.44
Mass -0.55 -0.65 -0.56 -0.59 -0.64 -0.58 1 0.75 0.77 0.76
Beak.Length_Culmen -0.5 -0.6 -0.51 -0.5 -0.6 -0.57 0.75 1 0.4 0.45
Beak.Depth -0.39 -0.5 -0.47 -0.46 -0.48 -0.43 0.77 0.4 1 0.94
Beak.Width -0.4 -0.51 -0.48 -0.46 -0.48 -0.44 0.76 0.45 0.94 1
F0_min F0_mean F0_max DF_min DF_mean DF_max Mass Beak.Length_Culmen Beak.Depth Beak.Width
1.0 0.8 0.6 0.4 0.2 0.0 −0.2 −0.4 −0.6

## II. Full phylogenetic tree of the 'All Birds' data (n = 77)

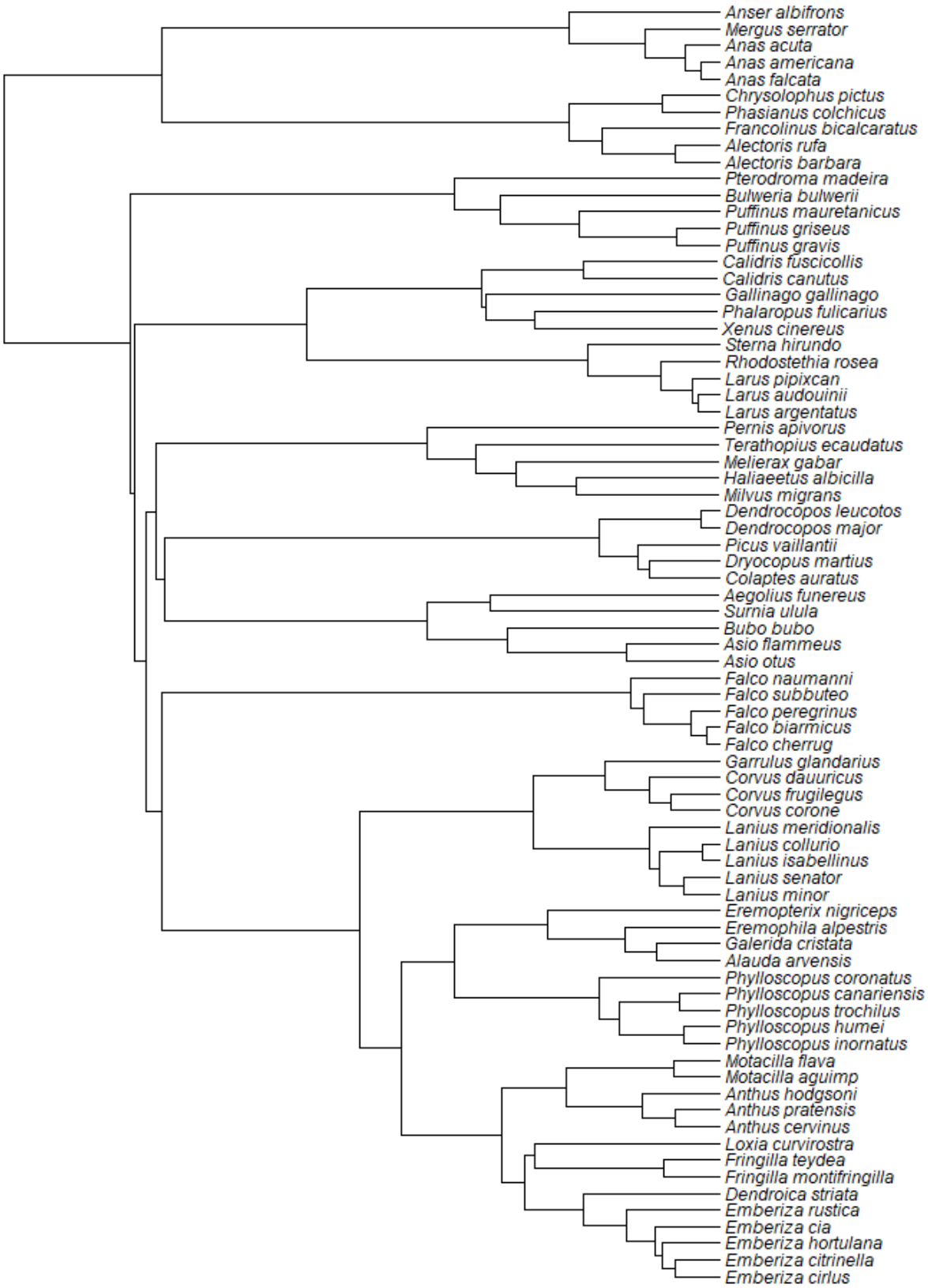

**III. $f_0$ mean vs DF mean – species labelled by order or family**

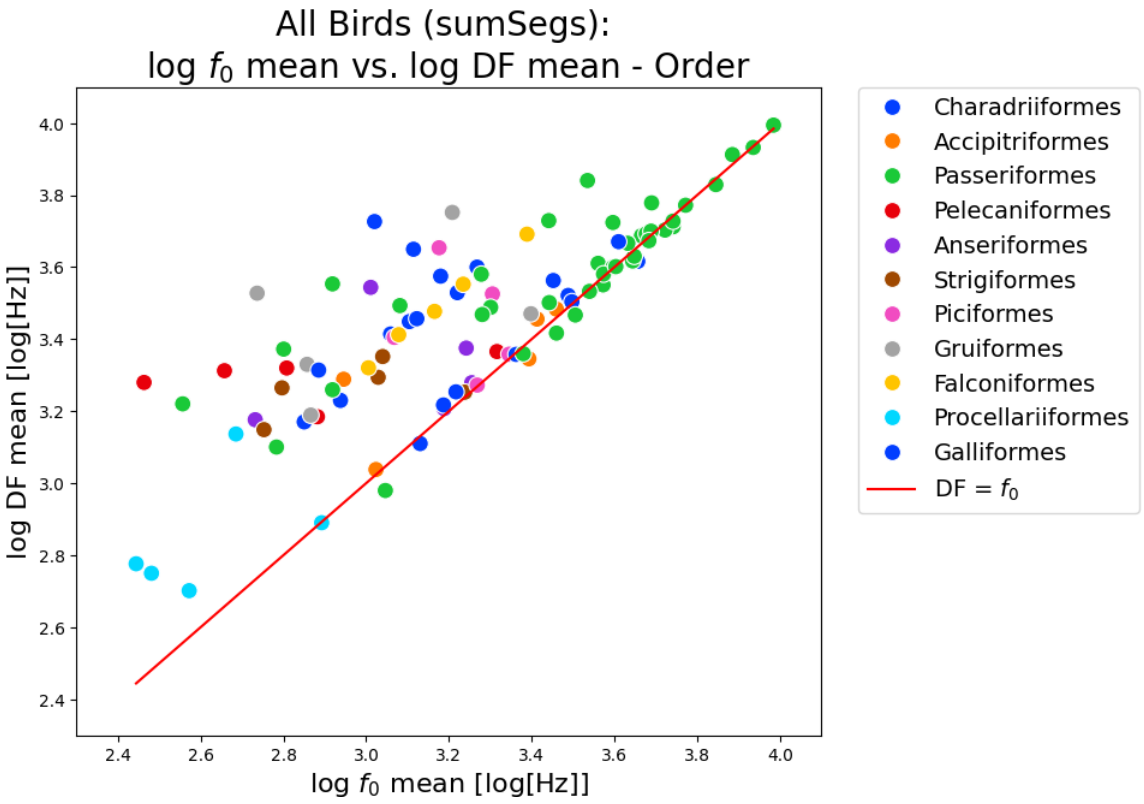


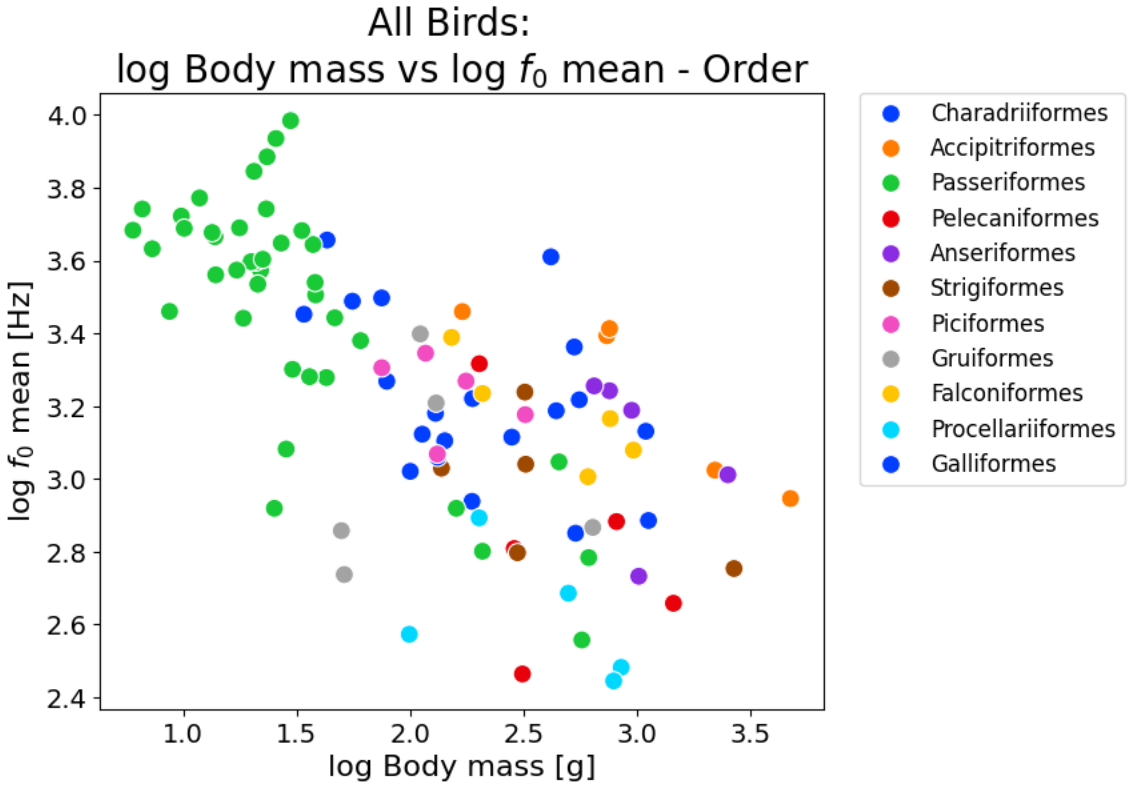

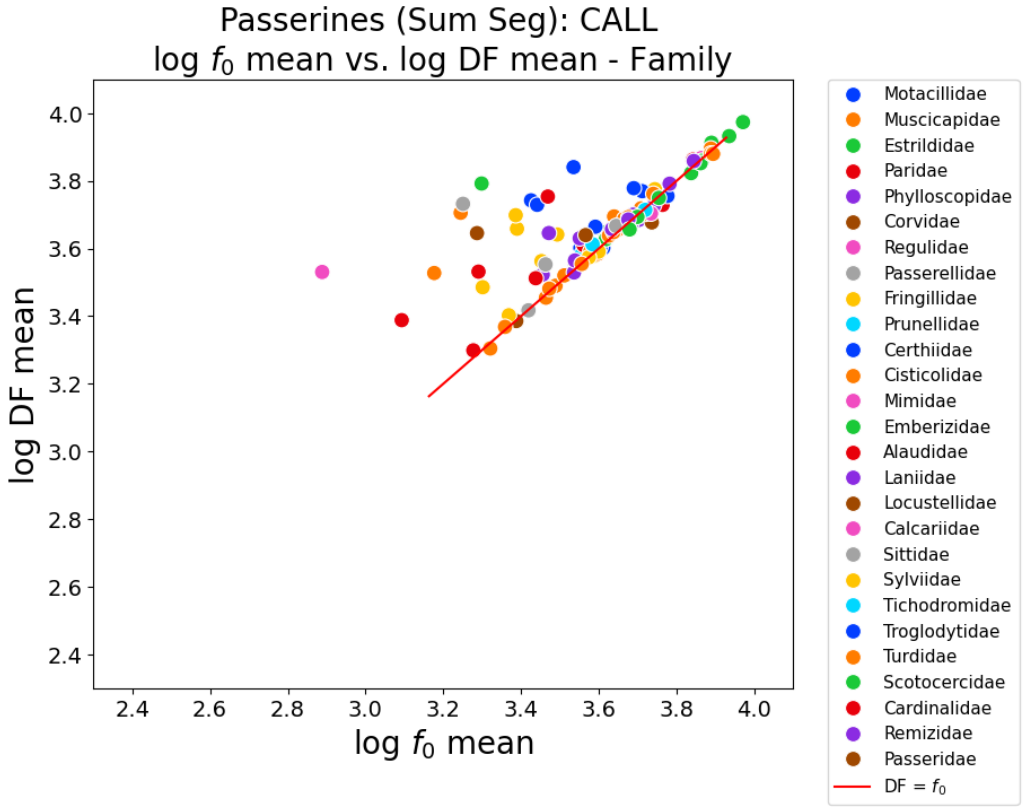
Passerines (Sum Seg): CALL
log $f_0$ mean vs. log DF mean - Family
log DF mean
log $f_0$ mean
4.0
3.8
3.6
3.4
3.2
3.0
2.8
2.6
2.4
2.4
2.6
2.8
3.0
3.2
3.4
3.6
3.8
4.0
Motacillidae
Muscicapidae
Estrildidae
Paridae
Phylloscopidae
Corvidae
Regulidae
Passerellidae
Fringillidae
Prunellidae
Certhiidae
Cisticolidae
Mimidae
Emberizidae
Alaudidae
Laniidae
Locustellidae
Calcariidae
Sittidae
Sylviidae
Tichodromidae
Troglodytidae
Turdidae
Scotocercidae
Cardinalidae
Remizidae
Passeridae
DF = $f_0$

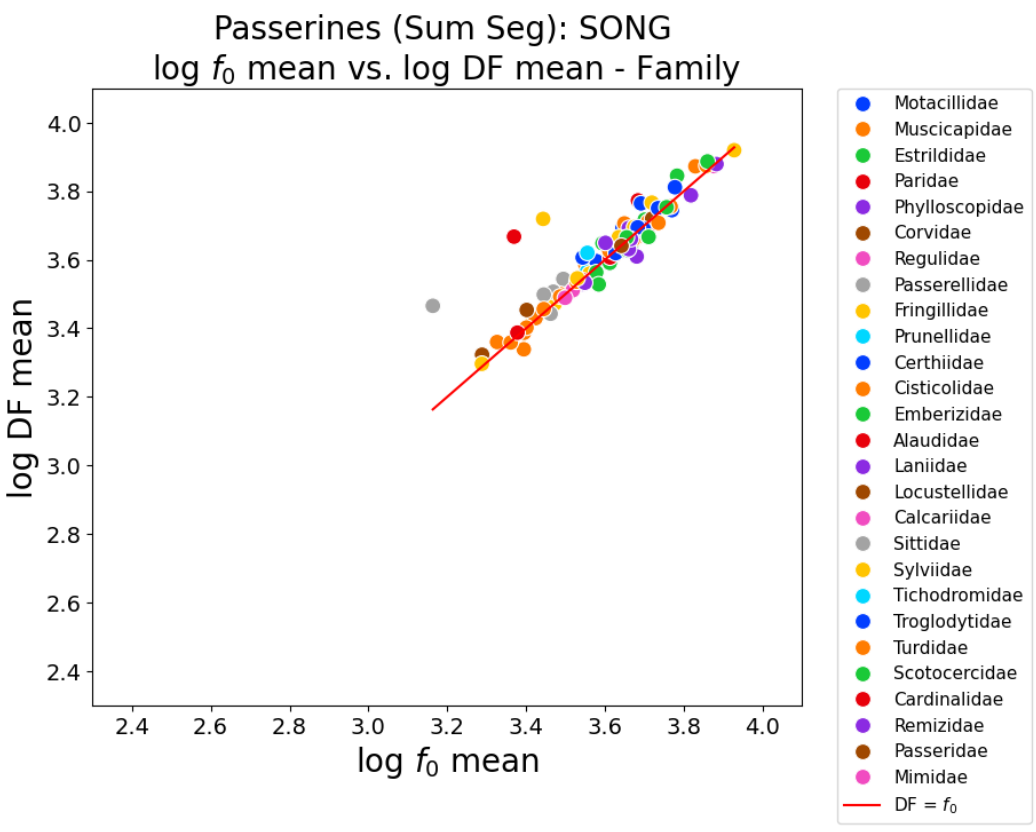
Passerines (Sum Seg): SONG
log $f_0$ mean vs. log DF mean - Family
log DF mean
log $f_0$ mean
4.0
3.8
3.6
3.4
3.2
3.0
2.8
2.6
2.4
2.4
2.6
2.8
3.0
3.2
3.4
3.6
3.8
4.0
Motacillidae
Muscicapidae
Estrildidae
Paridae
Phylloscopidae
Corvidae
Regulidae
Passerellidae
Fringillidae
Prunellidae
Certhiidae
Cisticolidae
Emberizidae
Alaudidae
Laniidae
Locustellidae
Calcariidae
Sittidae
Sylviidae
Tichodromidae
Troglodytidae
Turdidae
Scotocercidae
Cardinalidae
Remizidae
Passeridae
Mimidae
DF = $f_0$

## IV. Full datasets with frequency mean measurements

**Songbirds dataset**

| Species | Species_engl | Family | $f_0$ mean CALL | DF mean CALL | $f_0$ mean SONG | DF mean SONG |
|---|---|---|---|---|---|---|
| ammomanes_cincturus | bar-tailedlark | Alaudidae | 1239 | 2444 | 2341 | 4649 |
| eremalauda_dunni | dunn'slark | Alaudidae | 1894 | 1990 | 3510 | 3463 |
| eremopterix_nigriceps | black-crownedsparrow-lark | Alaudidae | 3637 | 4079 | 4917 | 4766 |
| eremophila_bilopha | temminck'slark | Alaudidae | 4741 | 4877 | 4433 | 4296 |
| eremophila_alpestris | hornedlark | Alaudidae | 4957 | 4967 | 4301 | 4333 |
| melanocorypha_leucoptera | white-wingedlark | Alaudidae | 2740 | 3252 | 4101 | 4043 |
| plectrophenax_nivalis | snowbunting | Calcariidae | 5422 | 5053 | 3299 | 3244 |
| pheucticus_ludovicianus | rose-breastedgrosbeak | Cardinalidae | 2944 | 5670 | 2388 | 2440 |
| certhia_brachydactyla | short-toedtreecreeper | Certhiidae | 5533 | 5441 | 5887 | 5555 |
| cisticola_juncidis | zittingcisticola | Cisticolidae | 4359 | 4952 | 6750 | 7456 |
| prinia_gracilis | gracefulprinia | Cisticolidae | 5500 | 5776 | 5441 | 5101 |
| pica_pica | magpie | Corvidae | 2442 | 2429 | 1942 | 2103 |
| emberiza_citrinella | yellowhammer | Emberizidae | 9354 | 9413 | 6067 | 7000 |
| emberiza_cirlus | cirlbunting | Emberizidae | 8619 | 8557 | 4095 | 3898 |
| emberiza_cineracea | cinereousbunting | Emberizidae | 4149 | 4242 | 4122 | 4029 |
| emberiza_cia | rockbunting | Emberizidae | 7760 | 8179 | 5706 | 5664 |
| emberiza_aureola | yellow-breastedbunting | Emberizidae | 7329 | 7233 | 3782 | 3659 |
| emberiza_rustica | rusticbunting | Emberizidae | 7274 | 7116 | 3839 | 3374 |
| emberiza_leucocephalos | pinebunting | Emberizidae | 4300 | 4434 | 4669 | 4458 |
| emberiza_pusilla | littlebunting | Emberizidae | 6879 | 6650 | 4848 | 4668 |
| emberiza_buchanani | grey-neckedbunting | Emberizidae | 4600 | 4746 | 3925 | 4447 |
| emberiza_schoeniclus | reedbunting | Emberizidae | 5683 | 5618 | 5137 | 4641 |
| emberiza_bruniceps | red-headedbunting | Emberizidae | 4777 | 4534 | 4521 | 4628 |
| uraeginthus_bengalus | red-cheekedcordon-bleu | Estrildidae | 1989 | 6196 | 7245 | 7705 |
| lagonosticta_senegala | red-billedfirefinch | Estrildidae | 4131 | 4443 | 4671 | 4626 |
| amandava_amandava | redavadavat | Estrildidae | 5824 | 5877 | 5023 | 5210 |
| serinus_canaria | canary | Fringillidae | 3113 | 4379 | 4725 | 4959 |
| carduelis_carduelis | goldfinch | Fringillidae | 3884 | 3793 | 4125 | 4150 |
| dendroica_striata | blackpollwarbler | Fringillidae | 5861 | 5863 | 8468 | 8308 |
| carduelis_cannabina | linnet | Fringillidae | 2453 | 4556 | 2774 | 5238 |
| pinicola_enucleator | pinegrosbeak | Fringillidae | 2337 | 2527 | 2970 | 2966 |
| fringilla_teydea | bluechaffinch | Fringillidae | 2001 | 3059 | 2617 | 2674 |
| dendroica_palmarum | palmwarbler | Fringillidae | 5550 | 5961 | 5236 | 5841 |
| carduelis_chloris | greenfinch | Fringillidae | 2835 | 3654 | 3642 | 3626 |
| lanius_minor | lessergreyshrike | Laniidae | 2856 | 3333 | 3486 | 3380 |
| locustella_naevia | grasshopperwarbler | Locustellidae | 5449 | 4755 | 5245 | 5249 |
| dumetella_carolinensis | catbird | Mimidae | 774 | 3393 | 3153 | 3083 |
| motacilla_aguimp | africanwagtail | Motacillidae | 3901 | 4618 | 4151 | 4389 |
| motacilla_citreola | citrinewagtail | Motacillidae | 5150 | 5881 | 5429 | 5629 |
| motacilla_flava | yellowwagtail | Motacillidae | 4897 | 6004 | 5990 | 6480 |
| anthus_richardi | richard'spipit | Motacillidae | 4089 | 3998 | 4408 | 4921 |
| anthus_spinoletta | waterpipit | Motacillidae | 2666 | 5525 | 3495 | 4041 |
| anthus_campestris | tawnypipit | Motacillidae | 4017 | 4014 | 3784 | 3945 |
| anthus_petrosus | rockpipit | Motacillidae | 3570 | 4000 | 4913 | 5813 |
| anthus_pratensis | meadowpipit | Motacillidae | 2763 | 5360 | 4239 | 4162 |
| anthus_hodgsoni | olive-backedpipit | Motacillidae | 3428 | 6928 | 4821 | 4950 |
| tarsiger_cyanurus | red-flankedbluetail | Muscicapidae | 4747 | 4930 | 3375 | 3437 |
| monticola_solitarius | bluerockthrush | Muscicapidae | 3600 | 3585 | 3065 | 3110 |
| phoenicurus_phoenicurus | redstart | Muscicapidae | 3788 | 3905 | 4084 | 4227 |
| phoenicurus_moussieri | moussier'sredstart | Muscicapidae | 4342 | 4450 | 4686 | 4547 |
| oenanthe_leucura | blackwheatear | Muscicapidae | 3960 | 3844 | 3058 | 3163 |
| muscicapa_striata | spottedflycatcher | Muscicapidae | 7732 | 7595 | 7204 | 7491 |

| | | | | | | |
|---|---|---|---|---|---|---|
| myrmecocichla_aethiops | northernanteaterchat | Muscicapidae | 3246 | 3315 | 2785 | 2858 |
| ficedula_semitorquata | semi-collaredflycatcher | Muscicapidae | 4450 | 4526 | 5136 | 4995 |
| luscinia_svecica | bluethroat | Muscicapidae | 3756 | 3924 | 4201 | 4105 |
| monticola_saxatilis | rockthrush | Muscicapidae | 3083 | 3089 | 3289 | 3239 |
| oenanthe_isabellina | isabellinewheatear | Muscicapidae | 4715 | 4876 | 3551 | 3849 |
| oenanthe_hispanica | black-earedwheatear | Muscicapidae | 4229 | 4349 | 3372 | 3372 |
| erithacus_rubecula | robin | Muscicapidae | 7729 | 7860 | 4459 | 5081 |
| ficedula_albicollis | collaredflycatcher | Muscicapidae | 5112 | 5232 | 5126 | 5145 |
| ficedula_hypoleuca | piedflycatcher | Muscicapidae | 4629 | 4867 | 4455 | 4506 |
| ficedula_parva | red-breastedflycatcher | Muscicapidae | 1757 | 5077 | 4774 | 4616 |
| oenanthe_moesta | red-rumpedwheatear | Muscicapidae | 2969 | 3029 | 2120 | 2291 |
| muscicapa_dauurica | brownflycatcher | Muscicapidae | 5246 | 5046 | 5843 | 5693 |
| parus_ater | coaltit | Paridae | 5809 | 5358 | 4736 | 4734 |
| parus_teneriffae | canaryislandstit | Paridae | 1952 | 3401 | 5093 | 4808 |
| parus_palustris | marshtit | Paridae | 6954 | 7295 | 4828 | 5931 |
| pipilo_erythrophthalmus | rufous-sidedtowhee | Passerellidae | 3460 | 3579 | 3122 | 3499 |
| passer_moabiticus | deadseasparrow | Passeridae | 3683 | 4361 | 4383 | 4370 |
| montifringilla_nivalis | snowfinch | Passeridae | 1935 | 4420 | 2521 | 2841 |
| phylloscopus_sibilatrix | woodwarbler | Phylloscopidae | 3438 | 3382 | 3541 | 3411 |
| phylloscopus_trochiloides | greenishwarbler | Phylloscopidae | 5047 | 4840 | 5178 | 5147 |
| phylloscopus_bonelli | bonelli'swarbler | Phylloscopidae | 3556 | 4268 | 4792 | 4069 |
| phylloscopus_brehmii | iberianchiffchaff | Phylloscopidae | 4742 | 4849 | 3993 | 4460 |
| phylloscopus_humei | hume'sleafwarbler | Phylloscopidae | 4823 | 4714 | 7637 | 7569 |
| phylloscopus_proregulus | pallas'swarbler | Phylloscopidae | 2962 | 4422 | 4483 | 4616 |
| phylloscopus_neglectus | plainleafwarbler | Phylloscopidae | 6987 | 7221 | 4398 | 4241 |
| phylloscopus_canariensis | canaryislandschiffchaff | Phylloscopidae | 4305 | 4546 | 4576 | 4926 |
| phylloscopus_coronatus | easterncrownedwarbler | Phylloscopidae | 4876 | 5011 | 4578 | 4446 |
| phylloscopus_collybita | chiffchaff | Phylloscopidae | 3457 | 3670 | 4575 | 4276 |
| phylloscopus_inornatus | yellow-browedwarbler | Phylloscopidae | 5517 | 5342 | 6578 | 6138 |
| prunella_collaris | alpineaccentor | Prunellidae | 3604 | 3843 | 3585 | 3676 |
| prunella_modularis | dunnock | Prunellidae | 5241 | 5178 | 4894 | 4872 |
| regulus_ignicapillus | firecrest | Regulidae | 7311 | 7370 | 7513 | 7467 |
| remiz_pendulinus | pendulinetit | Remizidae | 6057 | 6189 | 4634 | 4577 |
| cettia_cetti | cetti'swarbler | Scotocercidae | 5004 | 4938 | 4539 | 4248 |
| sitta_europaea | nuthatch | Sittidae | 2625 | 2614 | 2945 | 3212 |
| sitta_krueperi | krüper'snuthatch | Sittidae | 1781 | 5397 | 1457 | 2921 |
| sitta_tephronota | easternrocknuthatch | Sittidae | 2904 | 3573 | 2785 | 3150 |
| sitta_neumayer | rocknuthatch | Sittidae | 4414 | 4642 | 2898 | 2770 |
| sylvia_sarda | marmora'swarbler | Sylviidae | 2434 | 4995 | 4317 | 4632 |
| sylvia_undata | dartfordwarbler | Sylviidae | 3753 | 3750 | 3388 | 3514 |
| sylvia_hortensis | orpheanwarbler | Sylviidae | 3977 | 3900 | 1940 | 1979 |
| tichodroma_muraria | wallcreeper | Tichodromidae | 3837 | 4098 | 3593 | 4171 |
| troglodytes_troglodytes | wren | Troglodytidae | 5980 | 5696 | 4996 | 4892 |
| turdus_viscivorus | mistlethrush | Turdidae | 7832 | 7581 | 2517 | 2524 |
| turdus_eunomus | duskythrush | Turdidae | 2285 | 2335 | 2482 | 2438 |
| turdus_naumanni | naumann'sthrush | Turdidae | 1502 | 3369 | 2478 | 2181 |
| turdus_torquatus | ringouzel | Turdidae | 2911 | 2849 | 2654 | 2689 |
| turdus_unicolor | tickell'sthrush | Turdidae | 2094 | 2016 | 2296 | 2283 |

## All Birds dataset

| Species | Species_engl | Order | Family | $f_0$_mean | DF mean |
|---|---|---|---|---|---|
| terathopius_ecaudatus | bateleur | Accipitriformes | Accipitridae | 1056 | 1092 |
| haliaeetus_albicilla | white-tailedeagle | Accipitriformes | Accipitridae | 882 | 1944 |
| micronisus_gabar | gabargoshawk | Accipitriformes | Accipitridae | 2881 | 3045 |
| milvus_migrans | blackkite | Accipitriformes | Accipitridae | 2474 | 2216 |
| pernis_apivorus | honeybuzzard | Accipitriformes | Accipitridae | 2588 | 2857 |
| eremophila_alpestris | hornedlark | Passeriformes | Alaudidae | 4813 | 4870 |
| galerida_cristata | crestedlark | Passeriformes | Alaudidae | 1898 | 3805 |
| eremopterix_nigriceps | black-crownedsparrow-lark | Passeriformes | Alaudidae | 3637 | 4079 |
| alauda_arvensis | skylark | Passeriformes | Alaudidae | 4406 | 4142 |
| alauda_razae | rasolark | Passeriformes | Alaudidae | 3739 | 3555 |
| anser_albifrons | white-frontedgoose | Anseriformes | Anatidae | 1026 | 3498 |
| mergus_serrator | red-breastedmerganser | Anseriformes | Anatidae | 540 | 1501 |
| anas_acuta | pintail | Anseriformes | Anatidae | 1543 | 1613 |
| anas_falcata | falcatedduck | Anseriformes | Anatidae | 1800 | 1902 |
| anas_americana | americanwigeon | Anseriformes | Anatidae | 1746 | 2373 |
| egretta_gularis | reefegret | Pelecaniformes | Ardeidae | 291 | 1905 |
| nycticorax_nycticorax | nightheron | Pelecaniformes | Ardeidae | 763 | 1530 |
| ardea_cinerea | greyheron | Pelecaniformes | Ardeidae | 455 | 2053 |
| butorides_striatus | striatedheron | Pelecaniformes | Ardeidae | 2071 | 2321 |
| ardeola_ralloides | squaccoheron | Pelecaniformes | Ardeidae | 643 | 2089 |
| charadrius_pecuarius | kittlitz'splover | Charadriiformes | Charadriidae | 2833 | 3655 |
| vanellus_spinosus | spur-wingedlapwing | Charadriiformes | Charadriidae | 1661 | 3382 |
| vanellus_leucurus | white-tailedlapwing | Charadriiformes | Charadriidae | 1146 | 2596 |
| charadrius_leschenaultii | greatersandplover | Charadriiformes | Charadriidae | 3142 | 3191 |
| vanellus_tectus | black-headedlapwing | Charadriiformes | Charadriidae | 1048 | 5328 |
| corvus_corone | carrioncrow | Passeriformes | Corvidae | 360 | 1661 |
| corvus_frugilegus | rook | Passeriformes | Corvidae | 1113 | 955 |
| corvus_rhipidurus | fan-tailedraven | Passeriformes | Corvidae | 607 | 1260 |
| corvus_dauuricus | daurianjackdaw | Passeriformes | Corvidae | 632 | 2357 |
| garrulus_glandarius | jay | Passeriformes | Corvidae | 830 | 1818 |
| emberiza_citrinella | yellowhammer | Passeriformes | Emberizidae | 9649 | 9871 |
| emberiza_cirlus | cirlbunting | Passeriformes | Emberizidae | 8619 | 8557 |
| emberiza_rustica | rusticbunting | Passeriformes | Emberizidae | 7001 | 6748 |
| emberiza_hortulana | ortolanbunting | Passeriformes | Emberizidae | 3953 | 3983 |
| emberiza_cia | rockbunting | Passeriformes | Emberizidae | 7676 | 8177 |
| falco_cherrug | sakerfalcon | Falconiformes | Falconidae | 1199 | 2585 |
| falco_naumanni | lesserkestrel | Falconiformes | Falconidae | 2448 | 4915 |
| falco_peregrinus | peregrinefalcon | Falconiformes | Falconidae | 1463 | 3001 |
| falco_subbuteo | hobby | Falconiformes | Falconidae | 1717 | 3570 |
| falco_biarmicus | lannerfalcon | Falconiformes | Falconidae | 1013 | 2092 |
| rhodopechys_sanguinea | crimson-wingedfinch | Passeriformes | Fringillidae | 3466 | 3410 |
| loxia_curvirostra | commoncrossbill | Passeriformes | Fringillidae | 3203 | 2931 |
| fringilla_teydea | bluechaffinch | Passeriformes | Fringillidae | 2000 | 3079 |
| fringilla_montifringilla | brambling | Passeriformes | Fringillidae | 5520 | 5154 |
| dendroica_striata | blackpollwarbler | Passeriformes | Fringillidae | 5916 | 5914 |
| lanius_minor | lessergreyshrike | Passeriformes | Laniidae | 2771 | 3173 |
| lanius_senator | woodchatshrike | Passeriformes | Laniidae | 1908 | 2940 |
| lanius_meridionalis | southerngreyshrike | Passeriformes | Laniidae | 2398 | 2289 |
| lanius_isabellinus | isabellineshrike | Passeriformes | Laniidae | 829 | 3577 |
| lanius_collurio | red-backedshrike | Passeriformes | Laniidae | 1207 | 3114 |
| sterna_hirundo | commontern | Charadriiformes | Laridae | 1514 | 3758 |
| larus_pipixcan | franklin'sgull | Charadriiformes | Laridae | 1302 | 4464 |
| larus_audouinii | audouin'sgull | Charadriiformes | Laridae | 709 | 1480 |

| | | | | | |
|---|---|---|---|---|---|
| larus_argentatus | herringgull | Charadriiformes | Laridae | 1351 | 1289 |
| rhodostethia_rosea | ross'sgull | Charadriiformes | Laridae | 867 | 1698 |
| anthus_cervinus | red-throatedpipit | Passeriformes | Motacillidae | 3948 | 5297 |
| anthus_hodgsoni | olive-backedpipit | Passeriformes | Motacillidae | 3428 | 6928 |
| motacilla_aguimp | africanwagtail | Passeriformes | Motacillidae | 4446 | 4269 |
| anthus_pratensis | meadowpipit | Passeriformes | Motacillidae | 2763 | 5360 |
| motacilla_flava | yellowwagtail | Passeriformes | Motacillidae | 4897 | 6004 |
| muscicapa_dauurica | brownflycatcher | Passeriformes | Muscicapidae | 5275 | 5046 |
| luscinia_svecica | bluethroat | Passeriformes | Muscicapidae | 3747 | 3810 |
| ficedula_hypoleuca | piedflycatcher | Passeriformes | Muscicapidae | 4629 | 4867 |
| tarsiger_cyanurus | red-flankedbluetail | Passeriformes | Muscicapidae | 4753 | 4927 |
| oenanthe_halophila | westernmourningwheatear | Passeriformes | Muscicapidae | 4013 | 3995 |
| chrysolophus_pictus | goldenpheasant | Galliformes | Phasianidae | 1649 | 1794 |
| alectoris_rufa | red-leggedpartridge | Galliformes | Phasianidae | 2303 | 2279 |
| francolinus_bicalcaratus | double-spurredfrancolin | Galliformes | Phasianidae | 1538 | 1649 |
| phasianus_colchicus | pheasant | Galliformes | Phasianidae | 768 | 2061 |
| alectoris_barbara | barbarypartridge | Galliformes | Phasianidae | 4074 | 4686 |
| phylloscopus_trochilus | willowwarbler | Passeriformes | Phylloscopidae | 2884 | 2611 |
| phylloscopus_canariensis | canaryislandschiffchaff | Passeriformes | Phylloscopidae | 4288 | 4637 |
| phylloscopus_coronatus | easterncrownedwarbler | Passeriformes | Phylloscopidae | 4882 | 5011 |
| phylloscopus_humei | hume'sleafwarbler | Passeriformes | Phylloscopidae | 4823 | 4714 |
| phylloscopus_inornatus | yellow-browedwarbler | Passeriformes | Phylloscopidae | 5517 | 5342 |
| dryocopus_martius | blackwoodpecker | Piciformes | Picidae | 1501 | 4507 |
| picus_vaillantii | levaillant'sgreenwoodpecker | Piciformes | Picidae | 1856 | 1873 |
| picoides_major | greatspottedwoodpecker | Piciformes | Picidae | 2020 | 3354 |
| picoides_leucotos | white-backedwoodpecker | Piciformes | Picidae | 2215 | 2281 |
| colaptes_auratus | northernflicker | Piciformes | Picidae | 1170 | 2541 |
| puffinus_gravis | greatshearwater | Procellariiformes | Procellariidae | 303 | 562 |
| puffinus_mauretanicus | balearicshearwater | Procellariiformes | Procellariidae | 485 | 1370 |
| puffinus_griseus | sootyshearwater | Procellariiformes | Procellariidae | 278 | 598 |
| pterodroma_madeira | zino'spetrel | Procellariiformes | Procellariidae | 781 | 777 |
| bulweria_bulwerii | bulwer'spetrel | Procellariiformes | Procellariidae | 374 | 503 |
| rallus_aquaticus | waterrail | Gruiformes | Rallidae | 2502 | 2955 |
| porzana_parva | littlecrake | Gruiformes | Rallidae | 720 | 2138 |
| fulica_americana | americancoot | Gruiformes | Rallidae | 735 | 1546 |
| gallinula_angulata | lessermoorhen | Gruiformes | Rallidae | 1616 | 5649 |
| porzana_marginalis | stripedcrake | Gruiformes | Rallidae | 545 | 3370 |
| xenus_cinereus | tereksandpiper | Charadriiformes | Scolopacidae | 1854 | 3982 |
| phalaropus_fulicarius | redphalarope | Charadriiformes | Scolopacidae | 3078 | 3322 |
| gallinago_gallinago | snipe | Charadriiformes | Scolopacidae | 1326 | 2864 |
| calidris_fuscicollis | white-rumpedsandpiper | Charadriiformes | Scolopacidae | 4533 | 4132 |
| calidris_canutus | knot | Charadriiformes | Scolopacidae | 1272 | 2811 |
| surnia_ulula | hawkowl | Strigiformes | Strigidae | 1731 | 1790 |
| bubo_bubo | eagleowl | Strigiformes | Strigidae | 567 | 1409 |
| asio_otus | long-earedowl | Strigiformes | Strigidae | 626 | 1840 |
| asio_flammeus | short-earedowl | Strigiformes | Strigidae | 1097 | 2248 |
| aegolius_funereus | tengmalm'sowl | Strigiformes | Strigidae | 1070 | 1969 |